A Multiclass Simulation-Based Dynamic Traffic Assignment Model for Mixed Traffic Flow of Connected and Autonomous Vehicles and Human-Driven Vehicles

Behzad Bamdad Mehrabani[a,b]*, Jakob Erdmann[c], Luca Sgambi[b], Seyedehsan Seyedabrishami[d], Maaike Snelder[e,f]

[a] *Transport and Mobility Leuven, Leuven, Belgium*

[b] *Louvain Research Institute for Landscape, Architecture, Built Environment (LAB), Université Catholique de Louvain, Louvain-la-Neuve, Belgium*

[c]*German Aerospace Centre (DLR), Berlin, Germany*

[d]*School of Civil Engineering, University of Sydney, Australia*

[e]*Transport & Planning Department, Delft University of Technology, Delft, Netherlands*

[f]*Netherlands Organization for Applied Scientific Research (TNO), The Hague, Netherlands*

[*]*Corresponding Author Email: behzad.bamdad@uclouvain.be*

A Multiclass Simulation-Based Dynamic Traffic Assignment Model for Mixed Traffic Flow of Connected and Autonomous Vehicles and Human-Driven Vehicles

Connected and Autonomous Vehicles (CAVs) may exhibit different driving and route choice behaviors compared to Human-Driven Vehicles (HDVs), which can result in a mixed traffic flow with multiple classes of route choice behavior. To effectively address this issue, it is necessary to solve the Multiclass Traffic Assignment Problem (TAP) for mixed traffic of CAVs and HDVs. However, most existing studies have relied on analytical solutions that are difficult to apply in real-world and large networks, especially in dynamic scenarios. Furthermore, simulation-based methods have not fully considered all of CAVs' potential capabilities and have made several different assumptions about their route choice behavior. This study presents an open-source solution framework for the multiclass simulation-based traffic assignment problem in mixed traffic of CAVs and HDVs. The proposed model assumes that CAVs follow system optimal principle with rerouting capabilities, while HDVs adhere to user equilibrium principle. It also considers the impact of CAVs on road capacity through distinct driving behavioral models at both micro and meso scales. The proposed model is demonstrated through three case studies, which show that as the penetration rate of CAVs increases, the total travel time for all vehicles decreases. This study bridges the gaps in previous research and provides a valuable tool that can consider several assumptions for better understanding the impact of CAVs on mixed traffic flow.

Keywords: Simulation-Based Traffic Assignment; Connected and Autonomous Vehicles (CAVs); Mixed Traffic Flow; Human Driven Vehicles (HDVs); Multiclass Traffic Assignment

Word Count: 9429

1- Introduction and Background

The advent of Connected and Autonomous Vehicles (CAVs) has brought about a significant transformation in the transportation industry. The technology powering CAVs consists of two key components: automation and connectivity. Automation involves integrating decision-making and control systems between humans and machines to operate the vehicle, ranging from level 0 (fully manual) to level 5 (complete autonomy). This hierarchy represents the degree of collaboration between humans and machines in vehicle control. The second feature, connectivity, enables the vehicle to communicate with various elements such as infrastructure (V2I), other vehicles (V2V), and pedestrians (V2P). While CAVs have yet to be widely adopted in transportation systems, extensive research has been conducted on their impact on transportation network performance. Although there are differing opinions on the effects of CAVs on road networks, they are expected to bring several benefits. From a traffic assignment perspective, CAVs may have the following impacts on mixed traffic: 1- Improved Road capacity: CAVs' automation enhances driving behavior, leading to improved road capacity. This, in turn, affects link travel times and influences the route choice of both CAVs and Human-Driven Vehicles (HDVs). 2- Different route choice principles: As traffic management centers can control CAVs, they have comprehensive information about the road network status. Consequently, CAVs can follow different route choice principles compared to HDVs. For example, they can adhere to System Optimal (SO) principles instead of User Equilibrium (UE). 3- Rerouting capability: Thanks to the connectivity feature, CAVs can promptly respond to traffic congestion or disruptions by adjusting their routes through rerouting capabilities, unlike other vehicle types.

While some studies, such as (Melson et al., 2018), have attempted to address the Traffic Assignment Problem (TAP) in the presence of CAVs, it is important to note that achieving a 100%

Penetration Rate (PR) of CAVs may take a considerable amount of time. Therefore, it is crucial to investigate the impacts at various PR levels of CAVs in mixed traffic scenarios. In the literature, multiclass traffic assignment models have been developed to solve the TAP in mixed traffic, focusing on examining the route choices of diverse users. This heterogeneity can manifest in different aspects, such as value of time, travel mode, travel disutility function, information quality, network topology, and various routing behavioral principles (Xie & Liu, 2022). The last category of heterogeneity, related to different routing behavioral principles, can be formulated as a multiclass traffic equilibrium, which was initially addressed by Harker (Harker, 1988). However, the multiclass traffic equilibrium considering CAVs and HDVs, each following distinct routing behavioral principles, is a relatively new problem that requires further investigation.

To facilitate this investigation, Table 1 presents a compilation of previous studies that have implemented or proposed frameworks for solving the multiclass TAP in mixed traffic of CAVs and HDVs. These studies tackle the multiclass TAP in mixed traffic conditions either by considering the impacts of mixed traffic flow on road capacity or by accounting for the divergent routing behavior between CAVs and HDVs. They can be analyzed from three perspectives: 1) the solution algorithm employed, 2) the extent of CAVs' impact, and 3) the assumptions made regarding CAVs.

Regarding the algorithm used to solve the multiclass TAP in mixed traffic, there are two primary categories of solutions: simulation-based models and analytical-based models. Upon examining Table 1, it becomes evident that the number of studies employing analytical-based methods is higher compared to those utilizing simulation-based techniques. Analytical models rely on mathematical equations to estimate traffic flow and commonly employ the Bureau of Public Roads (BPR) function to calculate link travel costs. However, due to their macro-scale nature,

these models struggle to accurately capture individual vehicle interactions, and their implementation in large-scale networks can be computationally intensive and complex (Gawron, 1999). On the other hand, simulation-based models utilize traffic simulators to replicate traffic flow dynamics and interactions at the micro and meso-levels, enabling a more detailed representation of the impacts of CAVs on road capacity (Saw et al., 2015). These models often incorporate distinct driving behaviors for CAVs, such as faster reaction times (Mansourianfar et al., 2021) or deterministic acceleration models (Fakhrmoosavi et al., 2020). Compared to analytical models, simulation-based models are considered more accurate as they can depict traffic flow propagation with greater detail, particularly in relation to CAVs.

In terms of the scope of their impacts, it can be argued that since CAVs have not yet fully entered the transportation network, each study has made its own assumptions regarding the effects of CAVs on transportation. A literature review reveals that the majority of existing studies on multiclass TAP of mixed traffic flow and CAVs have focused on either the impact of CAVs on road capacity, specifically their driving behavior (Aziz, 2019; Bahrami & Roorda, 2020; Ngoduy et al., 2021; F. Zhang et al., 2020), or on the difference in routing principles between CAVs and HDVs, either SO or UE (Bagloee et al., 2017; Chen et al., 2020; Hu et al., 2018; Li et al., 2018; Medina-Tapia & Robusté, 2019; Olia et al., 2016; Samimi Abianeh et al., 2020; Sorani & Bekhor, 2018; J. Wang et al., 2019; Xie & Liu, 2022; K. Zhang & Nie, 2018). While a few studies, such as Fakhrmoosavi et al. (Fakhrmoosavi et al., 2020), Liu et al. (Liu et al., 2019), and J. Wang et al. (J. Wang et al., 2021, 2022), have considered both the distinct route choice behavior of CAVs and their impact on road capacity, they do not solve the multiclass equilibrium problem. They assumed that CAVs and HDVs follow the same routing behavioral principle (e.g., both classes follow UE principles). Few studies solve the multiclass equilibrium TAP (mixture of SO users and UE users)

considering CAVs' impacts on road capacity (Guo et al., 2021; Mansourianfar et al., 2021; G. Wang et al., 2020). Also, less attention is paid to the effects of CAVs' rerouting capability in the multiclass equilibrium problem (Hu et al., 2018). For instance, Mansourianfar et al. 2021 (Mansourianfar et al., 2021) solved the multiclass equilibrium TAP by the simulation-based method. CAVs' impact on road capacity is modeled by applying modified parameters of a simplified car-following model in meso simulation. However, in Mansourianfar et al.'s work, CAVs' rerouting capability is not considered.

In terms of previous studies' assumptions about CAVs' route choice behavior, some researchers assume CAVs will follow the SO routines (Aziz, 2019; Bagloee et al., 2017; Chen et al., 2020; Guo et al., 2021; Li et al., 2018; Mansourianfar et al., 2021; Ngoduy et al., 2021; Sorani & Bekhor, 2018; G. Wang et al., 2020; K. Zhang & Nie, 2018), while others think CAVs will follow UE principles (Bahrami & Roorda, 2020; Samimi Abianeh et al., 2020; J. Wang et al., 2019, 2021; Xie & Liu, 2022; F. Zhang et al., 2020). Also, some studies model the deterministic route choice behavior of CAVs (G. Wang et al., 2020; J. Wang et al., 2019, 2021, 2022), and some others assume the stochastic route choice behavior for CAVs (Xie & Liu, 2022; F. Zhang et al., 2020).

To summarize, by reviewing previous articles on the solution framework of multiclass equilibrium TAP in mixed traffic flow, the following gaps can be expressed: 1- Most of the studies have used analytical solutions, which can be challenging in large dynamic real cases. 2- The solution frameworks capable of considering the impacts of CAVs on road capacity and the impacts of CAVs on route choice (multiclass equilibrium with the rerouting capability) are very rare. 3- There are no commonly accepted assumptions about the future route choice and driving behavior of CAVs.

Thus, this study fills these gaps by proposing a new open-source solution framework of the Multiclass Simulation-based Traffic Assignment Problem for the Mixed traffic flow of CAVs and HDVs (MS-TAP-M). This simulation-based solution framework considers the impact of CAVs on road capacity and the different route choice behavior of CAVs compared to HDVs (in micro and meso simulation scales). To address CAVs' impact on road capacity, modified parameters of car-following/lane-changing models (in microscale) and queuing model (in mesoscale) are utilized. Also, to distinguish between CAVs and HDVs in terms of route choice, it is assumed that HDVs follow UE while CAVs follow SO with rerouting capability. Given the open-source nature of the solution framework, it presents an opportunity to incorporate diverse assumptions pertaining to the driving behavior and route selection behavior of CAVs into this framework.

The structure of this paper is organized as follows: In Section 2, the notations and abbreviations used in this paper are presented. Section 3 outlines the methodology used, while Section 4 presents the numerical results obtained. Section 5, present the results of applying the proposed methodology on a large-scale road network. Finally, Section 6 concludes the paper.

[Table 1: Review of Previous Studies on Multiclass Traffic Assignment]

2- Notations and Abbreviations

The used notations are listed in Table 2.

[Table 2: Notations]

3- Methodology

In this section, the solution algorithm of MS-TAP-M is presented. The MS-TAP-M is defined as a dynamic TAP in which two vehicle classes exist. The vehicle classification consists of two

distinct categories: CAVs, adhering to the SO principle, and HDVs, adhering to the UE principle. This framework can consider the rerouting behavior of CAVs while solving the MS-TAP-M. Also, it considers CAVs' impact on road capacity by setting the modified parameters of driving behavior on micro and meso scales.

The simulation-based approach for TAP was first proposed by Mahmassani and Peeta in 1993 (Mahmassani & Peeta, 1993), followed by Peeta and Mahmassani in 1995 (Peeta & Mahmassani, 1995). Unlike analytical models that rely on mathematical closed-form solutions, this method employs an iterative procedure to find the equilibrium solution. In a single-class setting, such as when all users seek UE or SO, the path flow distribution is updated at each iteration based on a path-swapping algorithm. This reassignment process helps determine if the algorithm is progressing in the correct direction and leads to a more efficient path selection. After each iteration, a convergence criterion is calculated to determine if the algorithm has reached termination (Mehrabani et al., 2022). In this study, the framework provided by (Mahmassani & Peeta, 1993; Peeta & Mahmassani, 1995) has been developed to consider two classes of vehicles (CAVs and HDVs). Figure 1 depicts the solution framework for the MS-TAP-M, referred to as "duaIterateMix". The framework comprises two components, namely the Path Selection Procedure (PSP) and Dynamic Network Loading (DNL). The PSP employs Dijkstra's algorithm, while the DNL utilizes the Simulation of Urban Mobility (SUMO) (Lopez et al., 2018). SUMO is a robust, open-source microscopic traffic simulation package capable of handling large networks and can also simulate traffic at the mesoscopic level (DLR, 2023).

Let $G(V, A)$ be the directed traffic network, consisting of a set of links A (with elements $a \in A$) and a set of nodes V (with elements $v \in V$). The set of all HDVs and CAVs between all origin and destination pairs (travel demand) is represented by $\mathrm{D}_H(R, \mathrm{S})$ and $\mathrm{D}_C(R, \mathrm{S})$ respectively.

The set of all origin nodes is denoted by R (with elements $r \in R$) and the set of all destination nodes is denoted by S (with elements $s \in S$). $J_H(r,s)$ (with $J_H \in \mathrm{D}_H$) is the set of HDVs traveling from origin r to destination s. Similarly, $J_C(r,\mathrm{s})$ (with $J_C \in \mathrm{D}_H$) is the set of CAVs traveling from origin r to destination s. Thus, ${j_h}^{r-s}$ represents an HDV traveling from origin r to destination s, and ${j_c}^{r-s}$ represents a CAV traveling from origin r to destination s. The assignment of $\mathrm{D}_H(R,\mathrm{S})$ and $\mathrm{D}_C(R,\mathrm{S})$ to $G(V,A)$ is the defined problem. The computation of the multiclass equilibrium condition involves calculating the shortest routes and travel times through iterative simulations.

In each iteration i $(i \in I)$, a routing algorithm (Dijkstra) is first applied to the road network to determine alternative paths, $P_{j_c,i}^{r-s}$ and $P_{j_h,i}^{r-s}$, for each vehicle, ${j_c}^{r-s}$ and ${j_h}^{r-s}$. For each CAV (${j_c}^{r-s}$), the k-shortest paths are computed based on the previous iteration's Marginal Travel Time (MTT), $\bar{c}_a^{\,i-1}$. For each HDV (${j_h}^{r-s}$), the k-shortest paths are calculated based on the previous iteration's travel time, c_a^{i-1}. Then, a network loading model (Logit) is applied to the sets of alternative paths, $P_{j_c,i}^{r-s}\ and\ P_{j_h,i}^{r-s}$, to select a path for each vehicle type $p_{j_c,i}^{r-s}$ $\left(p_{j_c,i}^{r-s} \in P_{j_c,i}^{r-s}\right)$; $p_{j_h,i}^{r-s}$ $\left(p_{j_h,i}^{r-s} \in P_{j_h,i}^{r-s}\right)$. Finally, a swapping algorithm is used to reassign a portion of vehicles in each class from their current paths to alternative paths to improve the selected path over iterations. The adjusted selected path (final path) of each vehicle type, $p_{j_c,i}^{*,r-s}\ and\ p_{j_h,i}^{*,r-s}$, is then determined and sent to SUMO for traffic simulation. The traffic simulation can be performed either on microscopic or mesoscopic scales. On a microscale, the modified parameters of car-following and lane-changing models are implemented to consider the distinctions between CAVs' and HDVs' driving behavior. While on the mesoscale, the modified parameters of queuing model are used to distinguish between CAVs and HDVs. Besides, a predefined percentage of CAVs ($r_{j_c}^{i}$) reroute during simulation based on the current state of the traffic (this percentage remain constant during simulation). At the end of the simulation, SUMO calculates the current travel time of each link,

c_a^i. This is done by aggregating and averaging the travel times of all vehicles on each link during a defined interval (ζ: 900 s). The resulting travel times, c_a^i, are used as input for the next iteration. The process is repeated iteratively with the aim of minimizing total travel time (TTT).

[Figure 1: Framework of the MS-TAP-M]

3-1- Path Selection Procedure

The subsequent sections will provide a detailed discussion of the steps involved in the path selection procedure.

3-1-1- Calculation of Marginal Travel Times

In this framework, HDVs determine their path selections by utilizing the link travel times from the previous iteration, adhering to the UE principle. Conversely, CAVs make their decisions based on the link MTT, following the SO principle. The MTT is defined as "marginal contribution of an additional traveler on the a^{th} link to the TTT on this link." (Sheffi, 1985). There are two options available for calculating the path MTT: 1) global approximation, and 2) local approximation. The local approximation computes the path MTT by summing up the corresponding link MTTs. For this study, the researchers implemented a surrogate model of the link MTT to calculate the local approximation of the path MTT (Mehrabani et al., 2022):

$$\bar{c}_a^{\,i} = c_a^{i-1} + f_a^{i-1}\frac{c_a^{i-1} - c_a^{i-2}}{f_a^{i-1} - f_a^{i-2}} \quad (1)$$

The variable $\bar{c}_a^{\,i}$ represents the surrogate MTT of link a at simulation step i. The variables c_a^{i-1} and c_a^{i-2} represent the travel time, or cost, of link a at simulation steps $i-1$ and $i-2$, respectively. The variables f_a^{i-1} and f_a^{i-2} represent the traffic flow of link a at simulation steps $i-1$ and $i-2$, respectively. The first component can be explained by the average travel time on

link a. The second component address the effect of one additional user on all the other travelers. Therefore, these two components represent a surrogate model of MTT.

3-1-2- Route Choice Model

The route choice can be represented through two different models, either deterministic or stochastic. In the deterministic approach, an "all-or-nothing" process is used, where all the traffic between each O-D pair is assigned to the path with the shortest travel time. On the other hand, in the stochastic approach, the routes are selected based on probabilities using discrete choice models. The researchers in this study chose the stochastic approach for practical reasons. Firstly, the deterministic approach is highly sensitive to even small changes in flow. For example, in a simple network consisting of two parallel routes of equal length, the all-or-nothing procedure results in oscillating route choices because drivers always choose the shortest route, which is the route with fewer cars. As a result, the solution is unstable, even in a clear equilibrium scenario where each route is used by 50% of the vehicles (Gawron, 1999; Sheffi, 1985). Secondly, when there are multiple alternative routes with slightly different travel times, it may be reasonable to select a route other than the strictly shortest route to avoid congestion on that route. The stochastic route choice models apply a scale parameter and converge to the optimum solution sooner than the deterministic approach.

The logit model is utilized to analyze the various route options available to individual vehicles, specifically $P_{c,i}^{r-s}$ and $P_{h,i}^{r-s}$. For each vehicle, the k-shortest paths are considered as potential alternatives. The formulation of the logit model is presented as follows.

$$pr_{k,j_c}^{i};\ pr_{k,j_h}^{i} = \frac{\exp(-\theta C_k^i)}{\sum_1^K \exp(-\theta C_K^i)} \tag{2}$$

$$C_k^i = \sum\nolimits_{\boldsymbol{a} \in \boldsymbol{A}} \delta_{a,k}^i \, c_a^i \tag{3}$$

$$\delta_{a,p}^{i} = \begin{cases} 1 \; if \; link \; a \; is \; on \; path \; k \\ 0 \; otherwise \end{cases} \quad (4)$$

The variables pr_{k,j_c}^{i} and pr_{k,j_h}^{i} represent the probabilities of CAV j_c and HDV j_h selecting path k in iteration i. C_k^i is the travel time, or cost, of path k in iteration i. A logit model scale parameter, θ, is used in the route choice procedure to prevent solution oscillations and instabilities. Although this study mainly focuses on a stochastic solution for the traffic assignment problem, it is possible to obtain a deterministic solution using the proposed algorithm by setting the scale parameter to approach infinity.

3-1-3- Swapping Algorithm

For the reassignment of a fraction of vehicles at each iteration, the Probabilistic Swapping (PSwap) algorithm is used instead of the traditional Method of Successive Average (MSA). The decision to use PSwap was made due to the limitations of MSA, which were highlighted in a previous study by Sbayti et al. in 2007 (Sbayti et al., 2007). In the authors' previous work, the PSwap algorithm was tested against MSA and demonstrated improved performance (Mehrabani et al., 2022).

$$p_{j,i}^{*,r-s} = \begin{cases} p_{j,i}^{r-s} & if \; x \geq \rho_i \\ p_{j,i-1}^{*,r-s} & if \; x < \rho_i \end{cases} \quad (5)$$

The equation for $p_{j,i}^{*,r-s}$ includes several variables: $p_{j,i}^{r-s}$ represents the selected path by vehicle j in iteration i based on the current logit model, while $p_{j,i-1}^{*,r-s}$ refers to the final selected path by vehicle j in iteration $i-1$. Additionally, x is a random variable ranging from 0 to 1, and ρ_i is the sequence of step size in each iteration, which determines the probability of keeping the previous final selected path. The value of ρ_i is predetermined and calculated using the equation $\rho_i = \frac{i}{\gamma}$, where i denotes the iteration number and γ is a scale parameter that controls the speed of

convergence. Choosing a low value for γ results in faster convergence, but only a limited number of alternative paths will be explored by each vehicle. In contrast, a high value of γ slows down the convergence speed, but more alternative paths will be examined. For stochastic assignments, it is typically better to use higher values of γ. However, when dealing with large or medium-scale networks, waiting for a high number of iterations can be computationally expensive. In this study, the value of γ has been set to 10 for microscale networks and 50 for mesoscale networks.

3-2- Dynamic Network Loading

Dynamic network loading is the process of assigning travel demand, or O-D entries, to a network while considering the varying travel times on specific links. The loading is performed in a dynamic manner, considering real-time changes in traffic conditions. The SUMO software is utilized for this purpose, which is capable of handling both microscale and mesoscale networks.

3-2-1- Modelling CAVs and HDVs

In this section, it is specified how the traffic flow propagation for HDVs and CAVs has been modeled in the SUMO simulation. Additionally, it is explained how the distinction between the driving behavior of HDVs and CAVs has been considered in the simulation.

3-2-1-1- Microsimulation

In SUMO, the movement of vehicles is modelled using car-following and lane-changing models on the microscale. The method for modelling CAVs in this study is in line with the work of Lu et al. (Lu et al., 2020) and Karbasi et al. (Karbasi et al., 2022). The fundamental idea behind modelling the longitudinal movement of CAVs is that they have the same car-following model as HDVs, with some modifications to simulate the full automation feature of CAVs. Thanks to

automation technologies, CAVs have a shorter reaction time, allowing them to follow the leading vehicle with a smaller headway distance compared to HDVs. It is assumed that CAVs have a shorter time headway, a smaller minimum gap, and a faster acceleration than CAVs, and they can avoid collisions if the leading vehicle begins braking within their acceleration bounds (Karbasi et al., 2022; Lu et al., 2020). The parameters modified for CAVs in the Krauss car-following model (Krauss et al., 1997) are listed in Table 3.

[Table 3: Parameters of the car-following model in SUMO]

The LC2013 lane-changing model, as applied in the SUMO traffic simulation, governs the lateral movement of vehicles (Lopez et al., 2018). To reflect the different lane-changing behaviors of CAVs and HDVs, the model's parameters are adjusted. The most crucial parameter is *lcAssertive*, which indicates a vehicle's willingness to accept smaller gaps on the target lane (DLR, 2023). A higher value of *lcAssertive* indicates a more aggressive attitude towards shorter gaps, meaning that the vehicle is more willing to change lanes with smaller gaps. The value of *lcAssertive* is set to 0.7 for CAVs and 1.3 for HDVs. This reflects the differences in the lane-changing behavior between the two vehicle types. For more information on the selection of car-following and lane-changing parameters for CAVs, please refer to (Karbasi et al., 2022).

3-2-1-2- Mesosimulation

The mesoscopic model in SUMO is based on the research conducted by Eissfeldt (Eissfeldt, 2004). This model involves organizing vehicles in traffic queues, which is like the cell transmission model (Daganzo, 1995). The vehicles are generally released from the queues in the same order they entered, following the first-in-first-out principle (Amini et al., 2019). The model calculates the time it takes for a vehicle to travel from the queue by considering the traffic state in the current

and subsequent queues, the minimum travel time, and the stage of the intersection (e.g., red, green, yellow). There are four possible combinations of traffic states between consecutive segments: 1) when a vehicle travels from a free segment to another free segment, 2) when a vehicle travels from a free segment to a congested segment, 3) when a vehicle travels from a congested segment to a free segment, and 4) when a vehicle travels from a congested segment to another congested segment (DLR, 2023). For each of these combinations, the minimum headway between vehicles is calculated. The parameter τ is used to set the minimum headways between vehicles as a multiplier for each of the four possible combinations.

Although some research has explored using cell transmission models or simplified car-following models to model CAVs in mesoscale networks (Mansourianfar et al., 2021; Melson et al., 2018), to the best of the authors' knowledge, there has been no previous investigation of modeling CAVs using an Eissfeldt queuing model in the SUMO software. Thus, in this study, the authors adopt the same approach used to model CAVs on the microscale to model CAVs in mesoscale networks. Specifically, CAVs and HDVs are distinguished based on their queuing model parameters, with different minimum headway (τ) values applied to each vehicle class. The assumption is that CAVs can follow more efficiently between consecutive segments compared to HDVs, leading to a lower τ parameter value for CAVs (Yu et al., 2021). To ensure consistency between the mesoscopic and microsimulation results, the τ parameter is calibrated for both CAVs and HDVs to obtain a Fundamental Diagram (FD) that is consistent between the two scales. To begin the calibration process, the microsimulation parameters are set according to Table 3, and the mesosimulation parameters are based on Presinger's work (Presinger, 2021).

The comparison between the meso and micro scales was performed by conducting a micro simulation for each class of vehicles on a typical highway and extracting its FD. Then, for each

class of vehicles, the τ parameter was adjusted in the meso scale in such a way that it had the closest FD to the micro scale. This type of calibration of mesoscopic parameters is recommended by previous studies (Tympakianaki et al., 2022). After calibration and comparison of FDs between the micro and mesoscales, the authors find that the value of τ is 1.06 for HDVs and 0.79 for CAVs. The FDs generated at the meso and micro scales for CAVs and HDVs are shown in Figure 2 using the calibrated parameters. For further details on the parameters used in the mesoscopic simulation in SUMO and modeling CAVs in mesoscale, please refer to Amini et al. (Amini et al., 2019) and Mansourianfar et al. (Mansourianfar et al., 2021), respectively.

[Figure 2: HDVs and CAVs fundamental diagrams in micro and meso simulations]

3-2-2- Rerouting

One of the CAVs' potentials is that they are connected to each other and to a traffic management center (V2V and V2I); thus, they can send and receive real-time information about traffic conditions and each link's travel time. It is assumed that CAVs have the rerouting capability to address this feature in MS-TAP-M. The mechanism of rerouting in this study is that in the dynamic network loading step, a predefined percentage of CAVs ($r_{j_c}^{i}$) receive updated travel times both before insertion and periodically during movement in the network. According to this updated travel time, if they find a path shorter than the pre-selected path's travel time, they will change their path to the newly found shortest path.

3-3- Convergence Criterion

Due to the absence of a closed-form solution for simulation-based methods, it is not possible to mathematically prove the convergence of the algorithm. All convergence criteria only act as a stopping point for the algorithm. In previous studies on UE solutions, a gap function is calculated

to check for convergence. However, in multiclass traffic conditions where there are two types of vehicles, SO seeking CAVs and UE seeking HDVs, a different convergence criterion is necessary. In line with Mansourianfar et al.'s (Mansourianfar et al., 2021) research, this study proposes a hybrid gap function for algorithm convergence. The multiclass traffic assignment condition is deemed to be satisfied when the travel time experienced by HDVs (UE-seeking) and the marginal travel time experienced by CAVs (SO-seeking) for the same origin-destination (O-D) pair are both minimal and equal. A relative gap is calculated for each vehicle class, and the algorithm is considered converged if the average of these two gaps becomes constant and falls below ε.

$$Gap_1(i) = \frac{\sum_{H\in D_H}\left(\frac{\sum_{h\in H} tt_{j_h,i}^{r-s}}{\pi_H} - tt_{H,i}^{*,r-s}\right)}{\delta_H} \tag{6}$$

$$Gap_2(i) = \frac{\sum_{C\in D_C}\left(\frac{\sum_{c\in C} \overline{tt}_{j_c,i}^{r-s}}{\pi_C} - \overline{tt}_{C,i}^{*,r-s}\right)}{\delta_C} \tag{7}$$

$$Hybrid\ Gap(i) = \frac{Gap_1(i) + Gap_2(i)}{2} \tag{8}$$

The notation used is as follows: $tt_{h,i}^{r-s}$ represents the travel time experienced by HDV j_h in iteration i, while traveling from origin r to destination s. $\overline{tt}_{c,i}^{r-s}$ represents the experienced marginal travel time of CAV j_c in iteration i, while traveling from origin r to destination s. Similarly, $tt_{H,i}^{*,r-s}$ and $\overline{tt}_{C,i}^{*,r-s}$ represent the least experienced travel time by HDVs and least experienced marginal travel time by CAVs, respectively, in iteration i, while travel from origin r to destination s. These travel times are determined through simulation, encompassing the cumulative travel times of the individual links traversed by the vehicles to reach their respective destinations. Since CAVs adhere to system optimal, their experienced travel time (utilized for route selection) is equivalent to the average travel time associated with the link, augmented by the additional travel time contributed by an extra user (the marginal travel time). In addition, π_H and

π_C denote the number of HDVs and CAVs, respectively, traveling from origin r to destination s. Similarly, $\delta_H$and δ_C denote the number of HDVs and CAVs O-D pairs.

4- Numerical Results

The algorithm under consideration was tested on two distinct networks, which are illustrated in Figure 3: (a) Random network and (b) Sioux Falls network. The simulations are executed by an Intel(R) Core (TM) i5-9400H CPU processor with 16 GB RAM. The ensuing sections present the outcomes of the traffic simulations performed on the test networks. The scenarios that were modeled for each network are specified in Table 4.

[Figure 3: Test Networks]

[Table 4: Simulated Scenarios]

4-1- Random Network

A random network was created in SUMO, as illustrated in Figure 3 (a). The network consists of 278 edges and 100 intersections, with the length of each edge ranging from 200 to 1000 meters and featuring either one or two lanes. To simulate traffic for an hour, 7200 vehicles were randomly generated and dispersed throughout the network. Six different scenarios were simulated for this network, as shown in Table 4, to investigate the potential capabilities of CAVs. In this case study, it is assumed that CAVs have different route choices and driving behaviors. The distinct route choice behavior is considered by assuming that CAVs follow SO and can reroute. On the other hand, the specific driving behavior is addressed by modifying the relevant car-following and lane changing model's parameters, as explained in previous sections. A microsimulation was carried out, which converged after 10 iterations. The TTT for all vehicles in each iteration for each scenario is displayed in Figure 4.

[Figure 4: Convergence patterns for Random network]

Table 5 displays the results of the simulations carried out on the Random network. A quick look at the table reveals that as the PR of CAVs increases, the TTT of vehicles decreases. The percentage of TTT reduction compared to scenario 1 (0% PR of CAVs) ranges from 12.9% (for 10% PR of CAVs) to 48.9% (for 100% PR of CAVs). This finding indicates that if all vehicles have the full automation driving mode (100% PR of CAVs) and follow SO routines with 50% probability of rerouting, the TTT can be reduced by 48.9% compared to the scenario where no CAVs are present. Moreover, the simulations show an increasing trend of the average speed and a decreasing trend of the average distance traveled by vehicles as the PR of CAVs increases.

[Table 5: Simulation Results for Random Network]

Figure 5 illustrates the traffic volume (vehicles per hour) in the Random network at different PRs of CAVs where thicker links represents more PR of CAVs. The figure shows that as the PRs of CAVs increase, the number of medium-volume and high-volume links also increases. This observation can be attributed to two reasons. Firstly, as the number of CAVs increases, the capacity of links also increases, enabling them to accommodate more vehicles. Consequently, the links that form part of the vehicles' shortest paths experience higher traffic volumes. The second reason is that as CAVs follow the SO, they are dispersed throughout the entire network and make use of any spare capacity available. As the PR of CAVs increases, the volume of alternative routes for each O-D pair also increases. This results in a greater number of blue links in 100% PR of CAVs as compared to 0% PR of CAVs.

[Figure 5: Traffic Volume of Random Network in different Penetration Rate of CAVs]

The scenarios that have been studied so far for the random network are the scenarios in which we witness a reduction in TTT due to the combined impact of CAVs' different driving and

route choice behavior. To have an in-depth view of the impacts of CAVs on TTT, several other scenarios have been investigated. Twelve new scenarios are simulated which either consider CAVs' different route choice behavior or CAVs different driving behavior (2*6 scenario). These new simulations have been compared with the results of the scenarios that have been done so far. The results of this comparison are illustrated in Figure 6. In this figure, the TTT for three different categories of scenarios is shown. These categories include: 1-scenarios in which only CAVs' different route choice behavior is modeled (Route choice impact), 2-scenarios in which only CAVs' different driving behavior is modeled (Capacity impact), and 3-scenarios in which both CAVs' different route choice and driving behavior is considered (Combined impact). This figure also displays the amount of improvement in TTT for each of the scenarios mentioned above. By having a glance at Figure 6, it can be recognized that when CAVs have solely different route choice behavior in comparison to HDVs, they have the least improvement in TTT. However, when they have both different route choices and driving behavior, we observe the best improvement in TTT.

[Figure 6: Impact of CAVs on TTT for Different Setting of Route Choice and Driving Behavior (Random Network)]

One of the factors that is important in examining the travel time difference between CAVs and HDVs for decision makers and policymakers is the concept of travel time heterogeneity. Investigating the extent to which CAVs experience a better travel time compared to when only HDVs are present is crucial in understanding the overall impact of CAVs on the transportation system. This study assumes that CAVs follow system optimal and have safer and faster driving behavior. Therefore, it is expected that a percentage of vehicles will experience longer travel times compared to when CAVs are not present. To examine this issue, data related to travel time heterogeneity is presented in two figures: Figure 7 illustrates the percentage decrease in

experienced travel time by vehicles compared to the percentage of vehicles experiencing this reduced travel time, considering different PRs of CAVs. Additionally, Figure 8 shows the percentage of added travel time for the entire fleet of vehicles relative to the percentage of vehicles experiencing this additional travel time. Analyzing these figures reveals that when we have 20% CAV penetration, between 16% and 17.7% of vehicles experience a travel time that is 10% longer than when CAVs are not present. However, as the CAVs PR increases, this percentage decreases. By examining Figure 8 and Table 5, it can be concluded that when all vehicles in the network are CAVs, certain percentages experience travel times that are longer, such as 6.2% experiencing a 10% longer travel time, 3.1% experiencing a 20% longer travel time, 1.5% experiencing a 30% longer travel time, 1.1% experiencing a 40% longer travel time, 0.9% experiencing a 50% longer travel time, 0.6% experiencing a 60% longer travel time, 0.4% experiencing a 70% longer travel time, 0.3% experiencing an 80% longer travel time, and 0.3% experiencing a 90% longer travel time compared to when only HDVs are present. As a result, the overall travel time of the entire network improves by 48.9%. This figure can provide valuable insights for policymakers in implementing CAVs in road networks, which can be easily extracted through simulation methods.

[Figure 7: Travel Time Heterogeneity (Reduced Travel Time) (Random Network)]

[Figure 8: Travel Time Heterogeneity (Additional Travel Time) (Random Network)]

4-2- Sioux Falls Network

The second case study in the article employed the Sioux Falls network, which is displayed in Figure 3 (b). In this case, a total of 36,000 vehicles were simulated, with their origins and destinations determined according to the demand pattern described in LeBlanc's study (LeBlanc et al., 1975). Mesoscopic simulation was used for this case study, utilizing the mesoscopic feature of

SUMO. The study analyzed six different scenarios, and the convergence pattern for all scenarios (scenarios 1 to 6) is depicted in Figure 9. For the initial analysis, it was assumed that CAVs exhibit different driving and route choice behavior. CAVs follow SO with rerouting capability, while HDVs follow UE. Additionally, CAVs have a lower headway in the queuing model of meso simulation.

[Figure 9: Convergence patterns for Sioux Falls network]

The simulation results (Table 6) indicate that in the full automation scenario (scenario 6), the TTT has the minimum value in comparison with other PRs of CAVs. The percentage of TTT reduction varies between 8.2% to 27.2%. Also, the average speed and distance traveled rise as the PR of CAVs increases.

[Table 6: Simulation Results for Sioux Falls Network]

Figure 10 depicts the volume on the Sioux Falls network for different PRs of CAVs, categorized based on both colors and width, where thicker links indicate higher PR of CAVs. Analyzing the differences in traffic volumes, this figure reveals that vehicles are distributed throughout the entire network in scenarios with high PRs of CAVs, avoiding selfish routing. CAVs select unused links, minimizing the travel time for the entire network. Additionally, in scenarios with high PRs of CAVs, the links' capacity increases, which can lead to a higher number of links with high volume. The same links can service more vehicles in less time compared to scenarios with lower PRs of CAVs.

[Figure 10: Traffic Volume of Sioux Falls Network in different Penetration Rate of CAVs]

Just like in the previous case study, various scenarios were performed to examine the isolated impact of various CAV-related driving and route choice behaviors. The results are

presented in Figure 11. The improvement in TTT was observed in different settings of CAV impact, ranging from 10.1% for the isolated impact of CAV-specific route choice behavior, 20.2% for the isolated impact of CAV-specific driving behavior, and reaching a maximum of 27.2% for the combined impact of both CAV-specific route choice and driving behaviors.

[Figure 11: Impact of CAVs on TTT for Different Setting of Route Choice and Driving Behavior (Sioux Falls Network)]

In Figure 12, the amount of reduced travel time experienced by the vehicles when there are CAVs in the road network is shown. Additionally, Figure 13 illustrates the amount of added travel time experienced by vehicles when CAVs are present in the network. Analyzing Figure 12 reveals that when CAVs exhibit different route choice and driving behavior compared to HDVs, 17.1% of them experience a 10% improvement in their travel time. Furthermore, 12.8% experience a 20% improvement, 10.1% experience a 30% improvement, 7.4% experience a 40% improvement, 6.2% experience a 50% improvement, 5.1% experience a 60% improvement, 3.6% experience a 70% improvement, 2.6% experience an 80% improvement, 1.6% experience a 90% improvement, and finally, 0.4% experience a 100% improvement in their travel time compared to when all vehicles are HDVs. Additionally, examining Figure 13 indicates that when all vehicles are CAVs, only 0.2% of vehicles experience a travel time that is 90% longer than when CAVs are not present. Furthermore, 12.6% of vehicles only experience a travel time that is 10% longer than under 100%HDV conditions. These results can be highly valuable for analyzing the policy sensitivity in CAV PRs which is easily measured using the simulation-based method.

[Figure 12: Travel Time Heterogeneity (Reduced Travel Time) (Sioux Falls Network)]

[Figure 13: Travel Time Heterogeneity (Additional Travel Time) (Sioux Falls Network)]

5- Application for Large-Scale Networks

Given the proposed algorithm's key advantage and the general effectiveness of simulation-based algorithms in solving the MS-TAP-M problem for large-scale transportation networks, the proposed algorithm is also applied to address the MS-TAP-M problem for the Belgian road network. To create the Belgium road network in SUMO, network data is extracted from OpenStreetMap, including highways, provincial roads, and regional roads. To determine the travel demand in Belgium, a probabilistic travel demand model is employed. The authors have previously developed, calibrated, and validated this travel demand model in a prior article (Mehrabani et al., 2023), which is also utilized in this study. Seven scenarios are considered for this network, outlined in Table 7. The (meso) simulation duration spans three hours, during rush hours.

[Table 7: Simulated Scenarios for Belgium Road Network]

Figure 14 illustrates the convergence pattern under different PRs. Notably, the graph highlights that the scenario with 100% HDVs displays the largest hybrid gap, whereas the 100% CAV scenario exhibits the smallest hybrid gap. This observation suggests that having a network entirely composed of CAVs results in a reduced difference between the optimal and attained solutions.

[Figure 14: Convergence patterns for Belgium network]

To explore the influence of CAVs on travel time and network performance, Figure 15 and Table 8 have been presented. Upon reviewing the figure, it becomes evident that as the percentage of CAVs PR increases, the overall travel time of the network reduces. The degree of enhancement in the total travel time of the network when CAVs are present varies between 2.7% (at a PR of 10%) and 10.9% (at a PR of 100%). As seen in Table 8, to achieve convergence on the Belgium road network (which is a large-scale network) during the peak hours (with over 243,000 vehicles),

between 6.5 to 8 hours is required, which is an acceptable computational time considering the size of the network and the number of vehicles.

[Figure 15: Total travel time in different penetration rate of CAVs (Belgium Network) (min)]

[Table 8: Simulation Results for Belgium Network]

Figure 16 provides a more precise evaluation of the network's performance under varying levels of CAVs penetration. As depicted in the figure, the path selection pattern undergoes a change with an increase in CAVs penetration, leading to fluctuations in the number of vehicles on each highway. This suggests that the network volume varies at different levels of CAVs penetration, as traffic tends to opt for routes that minimize the overall travel time of the network.

[Figure 16: Traffic Volume of Belgium Network in different Penetration Rate of CAVs]

6- Conclusion

The advent of CAVs may transform the transportation sector soon. One key advantage of CAVs is their ability to have their route choices controlled by a traffic management center, setting them apart from HDVs. This could result in a scenario where different types of road users with varying road preferences coexist simultaneously. As a result, it is crucial to solve the traffic assignment problem for a mixture of CAVs and HDVs. This paper addresses this challenge by presenting a solution framework for the Multiclass Simulation-based Traffic Assignment Problem for the Mixed traffic flow of CAVs and HDVs (MS-TAP-M). The MS-TAP-M problem involves assigning two classes of vehicles, each with unique route preferences and driving behaviors. It is assumed that CAVs adhere to the SO principle and have the capability to reroute, while HDVs follow UE routine. To account for the impact of CAVs on road capacity, the study incorporates modified car-following/lane-changing models (microscale) and a queuing model (meso scale). The

solution framework is an iterative process that involves path selection and dynamic network loading. Starting from an initial solution, the framework updates the path flow distribution in each iteration using a path-swapping algorithm. At the end of each iteration, a convergence criterion is calculated to determine when the algorithm should terminate.

To the best of the authors' knowledge, the proposed solution framework for MS-TAP-M is the first open-source algorithm that can be executed in both micro and meso scale simulation. In summary, the contributions of this study are as follows:

1. Algorithmic Innovation: This paper introduces a dynamic simulation-based algorithm for solving the multiclass traffic assignment problem of mixed traffic flow. This algorithm is open-source and allows for simulating various assumptions related to CAVs. The advantage of the simulation-based algorithm over analytical-based algorithms is its ability to solve the traffic assignment problem in large-scale networks within an acceptable computational time.
2. Comprehensive Assumptions: The proposed algorithm integrates a diverse set of probabilistic assumptions for CAVs. These assumptions encompass various driving behaviors, route choice behaviors, and real-time information-based rerouting, which have not been thoroughly investigated in previous studies. By incorporating these assumptions, the algorithm significantly improves the accuracy of solving the traffic assignment problem in the presence of CAVs.
3. Methodological Advancements (PSP): This study introduces novel elements in different aspects of solving the multiclass traffic assignment problem. Firstly, a new surrogate model for estimating the Marginal Travel Time (MTT) in the multiclass traffic assignment problem is employed within the PSP step. Secondly, a new

swapping algorithm designed for multiclass traffic assignment is proposed. Lastly, a new hybrid gap for the termination criterion of the algorithm is presented, enhancing its efficiency and convergence.

4. Methodological Advancements (DNL): The algorithm is applicable at both the mesoscopic and microscopic levels. The micro-level DNL section considers distinct parameters for CAVs in car-following and lane changing models compared to HDVs. Furthermore, in the meso-level, mesoscopic model parameters for CAVs are calibrated, considering the microscopic model. As far as the authors are aware, this represents the first instance where mesoscopic simulation parameters have been calibrated specifically for CAVs in SUMO.

The solution framework is called "duaIterateMix" and is freely available under the EPLv2 license on GitHub at https://github.com/eclipse/sumo/blob/main/tools/assign/duaIterateMix.py. This tool can be used by researchers and decision-makers to investigate the impacts of CAVs on the road network under various scenarios. "duaIterateMix" supports different assumptions on CAVs' route choice and driving behavior, providing flexibility in analyzing the potential effects of CAVs on traffic flow.

This study assessed the effectiveness of the "duaIterateMix" algorithm in two case studies, one at the micro scale and two at the meso scale. The simulation results revealed that as the PR of CAVs in the network increased, the travel time of vehicles decreased. The most significant improvement in TTT was observed in scenarios where CAVs had both unique route choices and driving behaviors, with a 48.9% improvement in the Random network and a 27.2% improvement in the Sioux Falls network. The second most significant impact on TTT was seen in scenarios where CAVs had only different driving behaviors, resulting in a 32.6% improvement in the

Random network and a 20.2% improvement in the Sioux Falls network. In contrast, the smallest effect on TTT was observed in scenarios where CAVs had only unique route choice behaviors, resulting in a 15.8% improvement in the Random network and a 10.1% improvement in the Sioux Falls network. This study investigated travel time heterogeneity, yielding valuable insights into the extra and reduced travel time imposed by CAVs on all vehicles. Furthermore, the proposed algorithm was employed to solve MS-TAP-M in a large-scale network (Belgium). The results demonstrated acceptable computational time for such large-scale network.

These findings provide crucial knowledge regarding the potential impact of CAVs, and they can prove beneficial for researchers and decision-makers seeking to comprehend the implications of CAVs on transportation systems.

7- Author Contributions

Behzad Bamdad Mehrabani contributed to the conceptualization of the study, developed the methodology, conducted the investigation, curated the data, wrote the original draft, and created the visualizations. Jakob Erdmann assisted with the methodology, developed the software, validated the results, performed formal analysis, curated the data, and reviewed and edited the writing. Luca Sgambi contributed to the conceptualization of the study, validated the results, reviewed, and edited the writing, provided supervision, managed the project administration, and acquired the funding. Seyedehsan Seyedabrishami assisted with the methodology, validated the results, and reviewed and edited the writing. Maaike Snelder contributed to the conceptualization of the study, developed the methodology, validated the results, analyzed, and interpreted the data, and reviewed and edited the writing. All authors reviewed the results and approved the final version of the manuscript.

8- Funding

The corresponding author was supported by the Université catholique de Louvain under the ‘‘Fonds Speciaux de Recherche’’ and the “Erasmus +” programs.

9- References

Amini, S., Tilg, G., & Busch, F. (2019). Calibration of mesoscopic simulation models for urban corridors based on the macroscopic fundamental diagram. *HEART 2019: 8th Symposium of the European Association for Research in Transportation*.

Aziz, H. M. A. (2019). Energy and Mobility Impacts of System Optimal Dynamic Traffic Assignment for a Mixed Traffic of Legacy and Automated Vehicles. *Transportation Research Record*, *2673*(9), 389–406. https://doi.org/10.1177/0361198119845658

Bagloee, S. A., Sarvi, M., Patriksson, M., & Rajabifard, A. (2017). A Mixed User-Equilibrium and System-Optimal Traffic Flow for Connected Vehicles Stated as a Complementarity Problem. *Computer-Aided Civil and Infrastructure Engineering*, *32*(7), 562–580. https://doi.org/10.1111/mice.12261

Bahrami, S., & Roorda, M. J. (2020). Optimal traffic management policies for mixed human and automated traffic flows. *Transportation Research Part A: Policy and Practice*, *135*, 130–143. https://doi.org/10.1016/j.tra.2020.03.007

Chen, Z., Lin, X., Yin, Y., & Li, M. (2020). Path controlling of automated vehicles for system optimum on transportation networks with heterogeneous traffic stream. *Transportation Research Part C: Emerging Technologies*, *110*, 312–329. https://doi.org/10.1016/j.trc.2019.11.017

Daganzo, C. F. (1995). The cell transmission model, part II: Network traffic. *Transportation Research Part B*, *29*(2), 79–93. https://doi.org/10.1016/0191-2615(94)00022-R

DLR. (2023). *SUMO User Documentation*. https://sumo.dlr.de/docs/index.html

Eissfeldt, N. G. (2004). Vehicle-based modelling of traffic. Theory and application to environmental impact modelling. In *University of Cologne* (p. 199). Universität zu Köln.

Fakhrmoosavi, F., Saedi, R., Zockaie, A., & Talebpour, A. (2020). Impacts of Connected and Autonomous Vehicles on Traffic Flow with Heterogeneous Drivers Spatially Distributed over Large-Scale Networks. *Transportation Research Record*, *2674*(10), 817–830. https://doi.org/10.1177/0361198120940997

Gawron, C. (1999). *Simulation-based traffic assignment: Computing user equilibria in large street networks*. Universität zu Köln.

Guo, Q., Ban, X. (Jeff), & Aziz, H. M. A. (2021). Mixed traffic flow of human driven vehicles and automated vehicles on dynamic transportation networks. *Transportation Research Part C: Emerging Technologies*, *128*, 103159. https://doi.org/10.1016/j.trc.2021.103159

Harker, P. T. (1988). Multiple Equilibrium Behaviors on Networks. *Transportation Science*, *22*(1), 39–46. https://doi.org/10.1287/trsc.22.1.39

Hu, T. Y., Tong, C. C., Liao, T. Y., & Chen, L. W. (2018). Dynamic route choice behaviour and simulation-based dynamic traffic assignment model for mixed traffic flows. *KSCE Journal of Civil Engineering*, *22*(2), 813–822. https://doi.org/10.1007/s12205-017-1025-8

Jiang, Y., Szeto, W. Y., Long, J., & Han, K. (2016). Multi-class dynamic traffic assignment with physical queues: intersection-movement-based formulation and paradox. *Transportmetrica A: Transport Science*, *12*(10), 878–908.

Karbasi, A. H., Mehrabani, B. B., Cools, M., Sgambi, L., & Saffarzadeh, M. (2022). Comparison of Speed-Density Models in the Age of Connected and Automated Vehicles. *Transportation Research Record: Journal of the Transportation Research Board*, *in press*, 036119812211185. https://doi.org/10.1177/03611981221118531

Krauss, S., Wagner, P., & Gawron, C. (1997). Metastable states in a microscopic model of traffic flow. *Physical Review E - Statistical Physics, Plasmas, Fluids, and Related Interdisciplinary Topics*, *55*(5), 5597–5602. https://doi.org/10.1103/PhysRevE.55.5597

LeBlanc, L. J., Morlok, E. K., & Pierskalla, W. P. (1975). An efficient approach to solving the road network equilibrium traffic assignment problem. *Transportation Research*, *9*(5), 309–318. https://doi.org/10.1016/0041-1647(75)90030-1

Li, R., Liu, X., & Nie, Y. (Marco). (2018). Managing partially automated network traffic flow: Efficiency vs. stability. *Transportation Research Part B: Methodological*, *114*, 300–324. https://doi.org/10.1016/j.trb.2018.06.004

Liu, Z., Guo, J., Chen, L., Wei, Y., Huang, W., & Cao, J. (2019). Effect of dynamic route guidance on urban traffic network under Connected vehicle environment. *European Journal of Transport and Infrastructure Research*, *19*(2), 142–159.

Lopez, P. A., Behrisch, M., Bieker-Walz, L., Erdmann, J., Flotterod, Y. P., Hilbrich, R., Lucken, L., Rummel, J., Wagner, P., & Wiebner, E. (2018). Microscopic Traffic Simulation using SUMO. *IEEE Conference on Intelligent Transportation Systems, Proceedings, ITSC*, *2018-Novem*, 2575–2582. https://doi.org/10.1109/ITSC.2018.8569938

Lu, Q., Tettamanti, T., Hörcher, D., & Varga, I. (2020). The impact of autonomous vehicles on urban traffic network capacity: an experimental analysis by microscopic traffic simulation. *Transportation Letters*, *12*(8), 540–549. https://doi.org/10.1080/19427867.2019.1662561

Mahmassani, H., & Peeta, S. (1993). Network performance under system optimal and user equilibrium dynamic assignments: implications for advanced traveler information systems. *Transportation Research Record 1408*, *1408*, 83.

Mansourianfar, M. H., Gu, Z., Waller, S. T., & Saberi, M. (2021). Joint routing and pricing control in congested mixed autonomy networks. *Transportation Research Part C: Emerging Technologies*, *131*, 103338. https://doi.org/10.1016/j.trc.2021.103338

Medina-Tapia, M., & Robusté, F. (2019). Implementation of connected and autonomous vehicles in cities could have neutral effects on the total travel time costs: Modeling and analysis for a circular city. *Sustainability (Switzerland)*, *11*(2), 482. https://doi.org/10.3390/su11020482

Mehrabani, B. B., Erdmann, J., Sgambi, L., & Snelder, M. (2022). Proposing a Simulation-Based Dynamic System Optimal Traffic Assignment Algorithm for SUMO: An Approximation of Marginal Travel Time. *SUMO Conference Proceedings*, *3*, 121–143.

Mehrabani, B. B., Sgambi, L., Maerivoet, S., & Snelder, M. (2023). Development, Calibration, and Validation of a Large-Scale Traffic Simulation Model: Belgium Road Network. *SUMO Conference Proceedings*, *4*, 15–27.

Melson, C. L., Levin, M. W., Hammit, B. E., & Boyles, S. D. (2018). Dynamic traffic assignment of cooperative adaptive cruise control. *Transportation Research Part C: Emerging Technologies*, *90*, 114–133. https://doi.org/10.1016/j.trc.2018.03.002

Ngoduy, D., Hoang, N. H., Vu, H. L., & Watling, D. (2021). Multiclass dynamic system optimum solution for mixed traffic of human-driven and automated vehicles considering physical queues. *Transportation Research Part B: Methodological*, *145*, 56–79. https://doi.org/10.1016/j.trb.2020.12.008

Olia, A., Abdelgawad, H., Abdulhai, B., & Razavi, S. N. (2016). Assessing the Potential Impacts of Connected Vehicles: Mobility, Environmental, and Safety Perspectives. *Journal of Intelligent Transportation Systems: Technology, Planning, and Operations*, *20*(3), 229–243. https://doi.org/10.1080/15472450.2015.1062728

Peeta, S., & Mahmassani, H. S. (1995). System optimal and user equilibrium time-dependent traffic assignment in congested networks. *Annals of Operations Research*, *60*(1), 81–113. https://doi.org/10.1007/BF02031941

Presinger, D.-I. C. (2021). *Calibration and Validation of Mesoscopic Traffic Flow Simulation*. Graz University of Technology.

Samimi Abianeh, A., Burris, M., Talebpour, A., & Sinha, K. (2020). The impacts of connected vehicle technology on network-wide traffic operation and fuel consumption under various incident scenarios. *Transportation Planning and Technology*, *43*(3), 293–312. https://doi.org/10.1080/03081060.2020.1735752

Saw, K., Katti, B. K., & Joshi, G. (2015). Literature review of traffic assignment: static and dynamic. *International Journal of Transportation Engineering*, *2*(4), 339–347. https://doi.org/10.22119/IJTE.2015.10447

Sbayti, H., Lu, C. C., & Mahmassani, H. S. (2007). Efficient implementation of method of successive averages in simulation-based dynamic traffic assignment models for large-scale network applications. *Transportation Research Record*, *2029*(2029), 22–30. https://doi.org/10.3141/2029-03

Sheffi, Y. (1985). Urban Transportation Networks Prentice-Hall. In *Engelwood, New Jersey* (Vol. 6). Prentice-Hall, Englewood Cliffs, NJ.

Sorani, M., & Bekhor, S. (2018). *Transportation network equilibrium in presence of autonomous vehicles*. *d*(2017), 1–3.

Tympakianaki, A., Nogues, L., Casas, J., Brackstone, M., Oikonomou, M. G., Vlahogianni, E. I., Djukic, T., & Yannis, G. (2022). Autonomous vehicles in urban networks: a simulation-based assessment. *Transportation Research Record*, *2676*(10), 540–552.

Wang, G., Qi, H., Xu, H., & Ryu, S. (2020). A mixed behaviour equilibrium model with mode choice and its application to the endogenous demand of automated vehicles. *Journal of Management Science and Engineering*, *5*(4), 227–248. https://doi.org/10.1016/j.jmse.2020.05.003

Wang, J., Lu, L., Peeta, S., & He, Z. (2021). Optimal toll design problems under mixed traffic flow of human-driven vehicles and connected and autonomous vehicles. *Transportation Research Part C: Emerging Technologies*, *125*, 102952. https://doi.org/10.1016/j.trc.2020.102952

Wang, J., Peeta, S., & He, X. (2019). Multiclass traffic assignment model for mixed traffic flow of human-driven vehicles and connected and autonomous vehicles. *Transportation Research Part B: Methodological*, *126*, 139–168. https://doi.org/10.1016/j.trb.2019.05.022

Wang, J., Wang, W., Ren, G., & Yang, M. (2022). Worst-case traffic assignment model for mixed traffic flow of human-driven vehicles and connected and autonomous vehicles by factoring in the uncertain link capacity. *Transportation Research Part C: Emerging Technologies*, *140*, 103703. https://doi.org/10.1016/j.trc.2022.103703

Xie, T., & Liu, Y. (2022). Impact of connected and autonomous vehicle technology on market penetration and route choices. *Transportation Research Part C: Emerging Technologies*, *139*, 103646. https://doi.org/10.1016/j.trc.2022.103646

Yu, H., Jiang, R., He, Z., Zheng, Z., Li, L., Liu, R., & Chen, X. (2021). Automated vehicle-involved traffic flow studies: A survey of assumptions, models, speculations, and perspectives. *Transportation Research Part C: Emerging Technologies*, *127*, 103101. https://doi.org/10.1016/j.trc.2021.103101

Zhang, F., Lu, J., & Hu, X. (2020). Traffic Equilibrium for Mixed Traffic Flows of Human-Driven Vehicles and Connected and Autonomous Vehicles in Transportation Networks under Tradable Credit Scheme. *Journal of Advanced Transportation*, *2020*. https://doi.org/10.1155/2020/8498561

Zhang, K., & Nie, Y. (Marco). (2018). Mitigating the impact of selfish routing: An optimal-ratio control scheme (ORCS) inspired by autonomous driving. *Transportation Research Part C: Emerging Technologies*, *87*, 75–90. https://doi.org/10.1016/j.trc.2017.12.011

Table 1: Review of Previous Studies on Multiclass Traffic Assignment

Author	Goal of the Study	TA Method	TA Approach	Software	CAVs impacts on capacity
Olia et al. 2016	Assessing the impacts of CAVs	Simulation-Based (Micro)	DTA with rerouting capability (frequently rerouting for CAVs and infrequently rerouting for non-CAVs)	Paramics	No
Samimi Abianeh et al. 2020	Evaluation of the impacts of CAVs on incidents		DUE for CAVs and HDVs (considering rerouting capability for CAVs)	SUMO	
Liu et al. 2019	Evaluate the effect of route guidance under the CAV environment			Paramics	Yes
Hu et al. 2018	Presenting DTA for Mixed Traffic	Simulation-Based (Meso)	Multiclass equilibrium (DSO and DUE) with rerouting capability	DynaTAI WAN	No
Fakhrmoosavi et al. 2020	Observing the impacts of CAVs by adaptive fundamental diagrams		DTA with rerouting capability for CAVs	DYNAS MART-P	Yes
Mansourianfar et al. 2021	Proposing a joint routing and pricing control scheme		Multiclass equilibrium: DSO for CAVs (without rerouting) and DUE for HDVs	Aimsun	
Bamdad Mehrabani et al., 2023 (**Current study**)	Proposing an open-source solution framework for multiclass TAP in mixed traffic flow	Simulation-Based (Micro and Meso)	Multiclass equilibrium: DSO for CAVs (with rerouting) and DUE for HDVs	SUMO	Yes
J. Wang, Peeta, and He 2019	Providing a solution algorithm for multiclass traffic assignment	Variational Inequality-Based	Mixed static traffic assignment: cross-nested logit for HDVs and UE for CAVs	N.A.	No
Li, Liu, and Nie 2018	Providing a control Day-To-Day dynamical system to guide AVs		Multiclass equilibrium: UE for HDVs and SO for CAVs	Matlab	
K. Zhang and Nie 2018	Proposing a route control scheme		Multiclass equilibrium with multiclass users: UE for HDVs and SO for CAVs	Matlab	
Xie and Liu 2022	Quantify the impacts of CAV on the vehicle market and route choices		SUE with different perceived travel times for CAVs and HDVs	N.A.	No
G. Wang et al. 2020	Providing a combined mode-route choice model for CAVs-HDVs		Multiclass equilibrium: SUE for HDVs and SO for CAVs		Yes

Table 1: Review of Previous Studies on Multiclass Traffic Assignment

Author	Goal of the Study	TA Method	TA Approach	Software	CAVs impacts on capacity
Jiang et al. 2016	Capture multiple vehicle classes in a DTA model	Variational Inequality-Based	Dynamic User Optimal for cars and trucks	N.A	Yes
F. Zhang, Lu, and Hu 2020	Examining equilibrium for mixed traffic flows		SUE with different cost functions for CAVs and Non-CAVs		
J. Wang et al. 2021	Control the HDV using the CAV/toll lanes		Cross nested logit with elastic demand for HDVs; UE with elastic demand for CAVs		
J. Wang et al. 2022	proposing a worst-case mixed traffic assignment model		SUE for HDVs and UE for CAVs		
Bagloee et al. 2017	To highlight the benefit of the cooperative routing	Mathematical Programming	Multiclass equilibrium: UE for HDVs and SO for CAVs	GAMS	No
Sorani and Bekhor 2018	Evaluation in the presence of autonomous vehicles		Multiclass equilibrium: UE for HDVs and SO for CAVs	N.A.	
Medina-Tapia and Robusté 2019	Evaluating the effects of CAVs on a city road network		Static assignment with a modified cost function for CAVs and HDVs		
Chen et al. 2020	Develop a path-control scheme		Multiclass equilibrium: SO for CAVs and UE for HDVs	CPLEX	No
Aziz 2019	Develop a mathematical SO-DTA model for mixed traffic flow		SO for both CAVs and HDVs	N.A.	Yes
Bahrami and Roorda 2020	Providing management policies for CAVs		UE for CAVs and HDVs		
Guo, Ban, and Aziz 2021	Explore a system-level control mechanism of CAVs consisting of CAV and HDV		Multiclass equilibrium: DSO for CAVs and DUE for HDVs		
Ngoduy et al. 2021	Proposes a DSO formulation for the multiclass DTA problem		DSO for both HDVs and CAVs		

DSO: Dynamic System Optimal; DTA: Dynamic Traffic Assignment; DUE: Dynamic User Equilibrium; SUE: Stochastic User Equilibrium

Table 2: Notations

Indices	
f	index for traffic flow
i	index for iteration steps
k	index for path
j	index for vehicle
Sets	
$G(V, A)$	traffic network
$\mathrm{D}_H(R, \mathrm{S})$	set of all HDVs ($J_H \in \mathrm{D}_H$)
$\mathrm{D}_C(R, \mathrm{S})$	set of all CAVs ($J_C \in \mathrm{D}_H$)
$J_H(r, s)$	set of HDVs, travel from r to s ($j_h^{r-s} \in J_H$)
$J_C(r, \mathrm{s})$	set of CAVs, travel from r to s ($j_c^{r-s} \in J_C$)
A	set of links ($a \in A$)
V	set of nodes ($v \in V$)
R	set of origin nodes ($r \in R$)
S	set of all destination nodes ($s \in S$)
I	set of simulation iterations ($i \in I$)
δ_H	cardinality of set $\mathrm{D}_H(R, \mathrm{S})$: number of HDVs O-D pairs
δ_C	cardinality of set $\mathrm{D}_C(R, \mathrm{S})$: number of CAVs O-D pairs
π_H	cardinality of set $J_H(r, s)$: number of HDVs travel from r to s
π_C	cardinality of set $J_C(r, s)$: number of CAVs travel from r to s
$P_{j_h,i}^{r-s}$	set of alternative paths for HDV j_h^{r-s} in iteration i, travel from r to s
$P_{j_c,i}^{r-s}$	set of alternative paths for CAV j_c^{r-s} in iteration i, travel from r to s
Variables, parameters, and elements	
c_a^i	travel time of link a in iteration i
c_a^0	free flow travel time of link a
$\bar{c}_a^i$	marginal travel time of link a in iteration i
C_k^i	travel time of path k in iteration i
$tt_{j_h,i}^{r-s}$	experienced travel time of HDV j_h in iteration i, travel from r to s
$\bar{tt}_{j_c,i}^{r-s}$	experienced marginal travel time of CAV j_c in iteration i, travel from r to s
$tt_{H,i}^{*,r-s}$	least experienced travel time by HDVs in iteration i, travel from r to s
$\bar{tt}_{C,i}^{*,r-s}$	least experienced marginal travel time by CAVs in iteration i, travel from r to s
$p_{j_h,i}^{r-s}$	selected path for HDV j_h^{r-s} in iteration i, travel from r to s
$p_{j_c,i}^{r-s}$	selected path for CAV j_c^{r-s} in iteration i, travel from r to s
$p_{j_h,i}^{*,r-s}$	final selected path for HDV j_h^{r-s} in iteration i, travel from r to s
$p_{j_c,i}^{*,r-s}$	final selected path for CAV j_c^{r-s} in iteration i, travel from r to s
pr_{k,j_h}^i	probability of selecting path k by HDV j_h in iteration i
pr_{k,j_c}^i	probability of selecting path k by CAV j_c in iteration i
$r_{j_c}^i$	probability of rerouting by CAV j_c during simulation in iteration i
ζ	updating travel times of each link interval

Table 3: Parameters of the car-following model in SUMO

	Mingap (m)	Accel (m/s^2)	Decel (m/s^2)	Emergency Decel (m/s^2)	Sigma	Tau (s)
HDV	2.5	2.6	4.5	8	0.5	1.0
CAV	1.5	3.5	4.5	8	0	0.9

Mingap: the offset to the leading vehicle when standing in a jam (m).
Accel: the acceleration ability of vehicles (m/s^2).
Decel: the deceleration ability of vehicles (m/s^2).
Emergency Decel: the maximum deceleration ability of vehicles in case of emergency (m/s^2).
Sigma: the driver imperfection (between 0 and 1).
Tau: the driver's desired (minimum) time headway (s).

Table 4: Simulated Scenarios

Network	Scenario	CAVs Penetration Rate	HDVs Penetration Rate	CAVs Rerouting Probability	Modeling CAVs driving behavior	CAVs routing principle	HDVs routing principle
Random Network	1	0	100	0.5	yes	SO	UE
	2	20	80				
	3	40	60				
	4	60	40				
	5	80	20				
	6	100	0				
Sioux Falls Network	1	0	100				
	2	20	80				
	3	40	60				
	4	60	40				
	5	80	20				
	6	100	0				

Table 5: Simulation Results for Random Network

Scenario	Hybrid Gap	Total Travel Time (hr.)	Average Speed (km/h)	Average Distance Travelled (km)	TTT improvement (%)	Computation Time (min)
1	12.49	2509.88	29.2	6.6	-	12
2	10.53	2185.54	31	6.6	12.9	09
3	9.86	2092.5	32	6.6	16.6	08
4	8.12	1834.36	34	6.4	26.9	08
5	7.44	1696.94	35.4	6.5	32.3	07
6	5.91	1496.72	37.5	6.4	48.9	06

Table 6: Simulation Results for Sioux Falls Network

Scenario	Hybrid Gap	Total Travel Time (hr.)	Average Speed (km/h)	Average Distance Travelled (km)	TTT improvement (%)	Computation Time (min)
1	4.44	31111.94	43.56	8.2	-	14
2	3.41	28566.56	45.57	8.3	8.2	14
3	3.11	26670.89	46.87	8.3	14.3	15
4	2.83	25475.60	47.95	8.3	18.1	15
5	2.51	23862.69	49.17	8.4	23.3	16
6	2.12	22636.86	49.93	8.4	27.2	16

[Table 7: Simulated Scenarios for Belgium Road Network]

Network	Scenario	CAVs Penetration Rate	HDVs Penetration Rate	CAVs Rerouting Probability	Modeling CAVs driving behavior	CAVs routing principle	HDVs routing principle
Belgium Road Network	1	0	100	0.5	yes	SO	UE
	2	10	90				
	3	20	80				
	4	40	60				
	5	60	40				
	6	80	20				
	7	100	0				

[Table 8: Simulation Results for Belgium Network]

Scenario	Hybrid Gap	Total Travel Time (hr.)	Average Speed (km/h)	Average Distance Travelled (km)	TTT improvement (%)	Computation Time (min)
1	380	216401.63	72.8	61.58	-	391
2	279	210400.53	72	60.22	2.7	421
3	244	205615.14	72.4	59.94	7.9	448
4	229	203318.06	73.1	59.27	6.04	453
5	228	196748.17	74.2	59.27	9.08	467
6	227	195526.90	74.8	58.91	9.64	474
7	215	192646.34	75.2	58.41	10.97	484

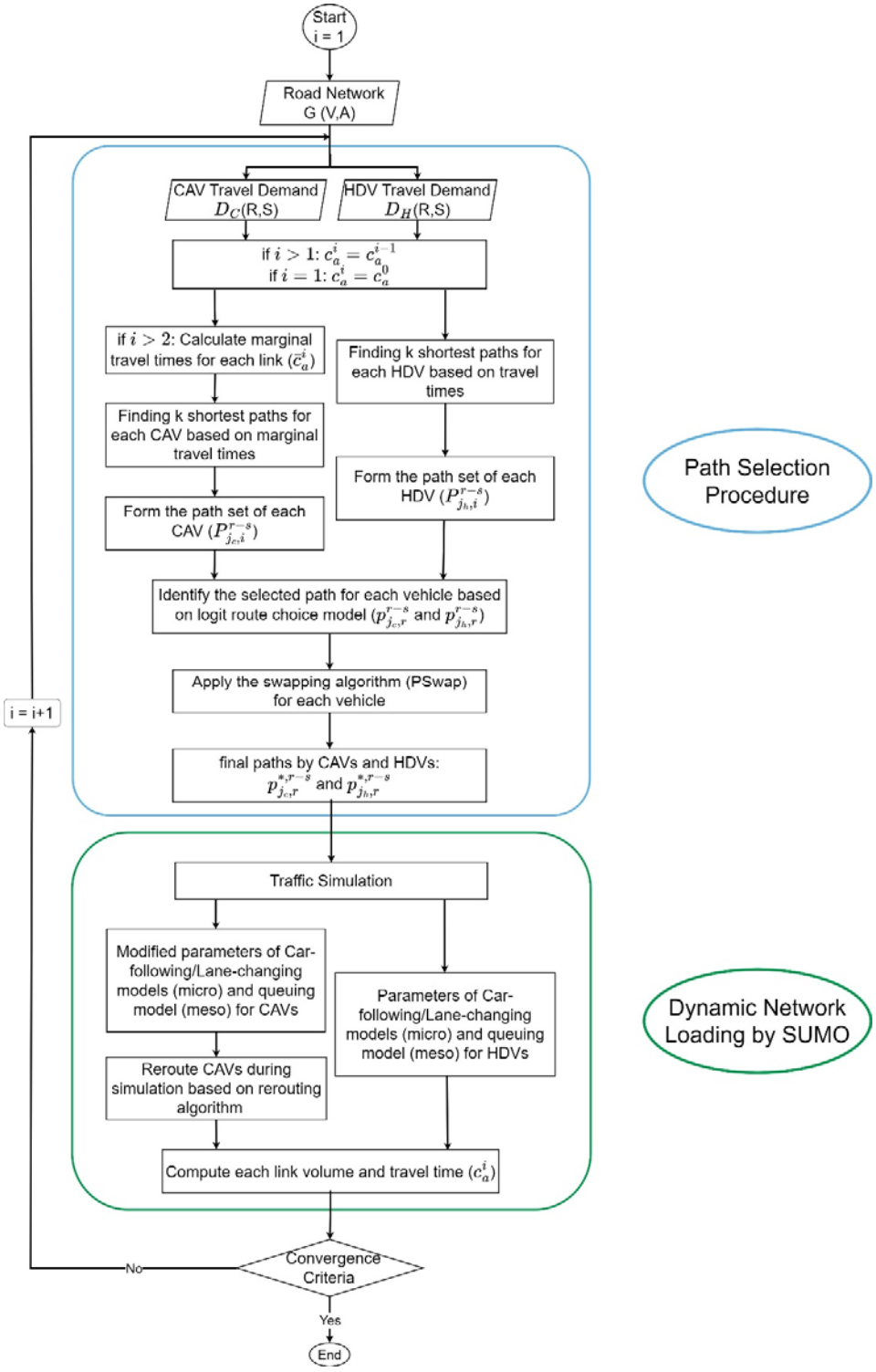
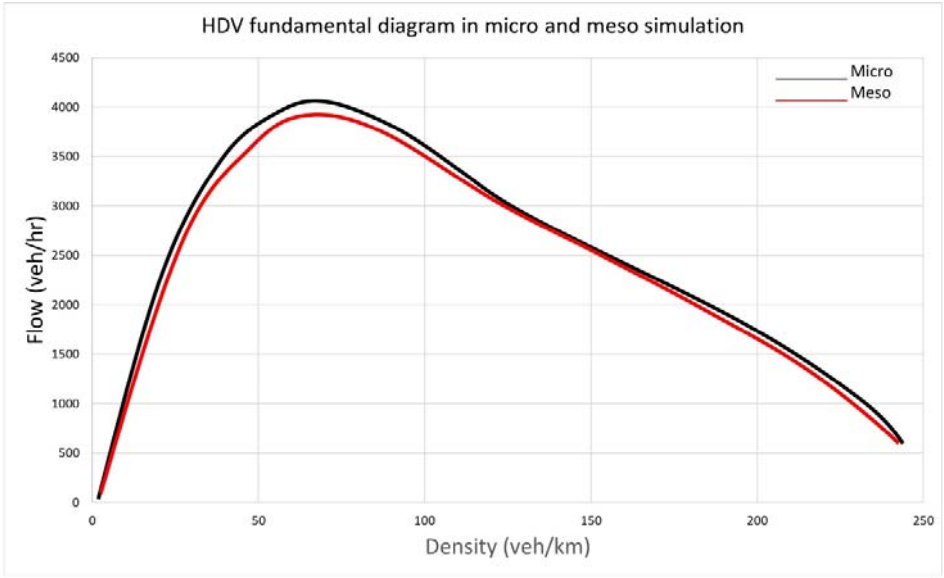

Start
i = 1
Road Network
G (V,A)
CAV Travel Demand
D_C(R,S)
HDV Travel Demand
D_H(R,S)
if $i > 1$: $c_a^i = c_a^{i-1}$
if $i = 1$: $c_a^i = c_a^0$
if $i > 2$: Calculate marginal travel times for each link ($\bar{c}_a^i$)
Finding k shortest paths for each HDV based on travel times
Finding k shortest paths for each CAV based on marginal travel times
Form the path set of each HDV ($P_{j_h,i}^{r-s}$)
Form the path set of each CAV ($P_{j_c,i}^{r-s}$)
Identify the selected path for each vehicle based on logit route choice model ($p_{j_c,r}^{r-s}$ and $p_{j_h,r}^{r-s}$)
Apply the swapping algorithm (PSwap) for each vehicle
final paths by CAVs and HDVs: $p_{j_c,r}^{*,r-s}$ and $p_{j_h,r}^{*,r-s}$
Path Selection Procedure
Traffic Simulation
Modified parameters of Car-following/Lane-changing models (micro) and queuing model (meso) for CAVs
Parameters of Car-following/Lane-changing models (micro) and queuing model (meso) for HDVs
Reroute CAVs during simulation based on rerouting algorithm
Compute each link volume and travel time (c_a^i)
Dynamic Network Loading by SUMO
Convergence Criteria
No
Yes
End
i = i+1

Figure 1


HDV fundamental diagram in micro and meso simulation
Micro
Meso
Flow (veh/hr)
Density (veh/km)
0
500
1000
1500
2000
2500
3000
3500
4000
4500
0
50
100
150
200
250

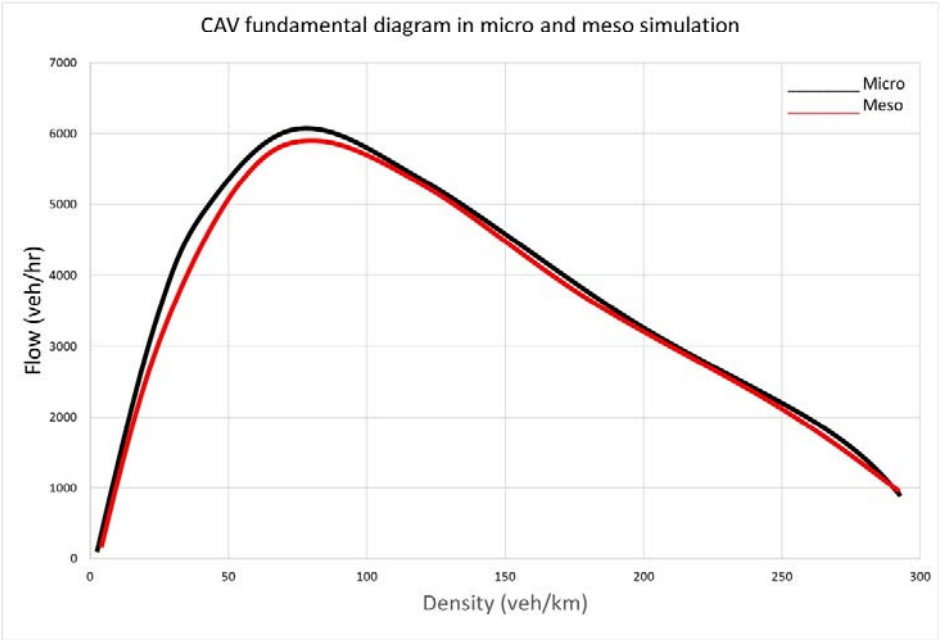
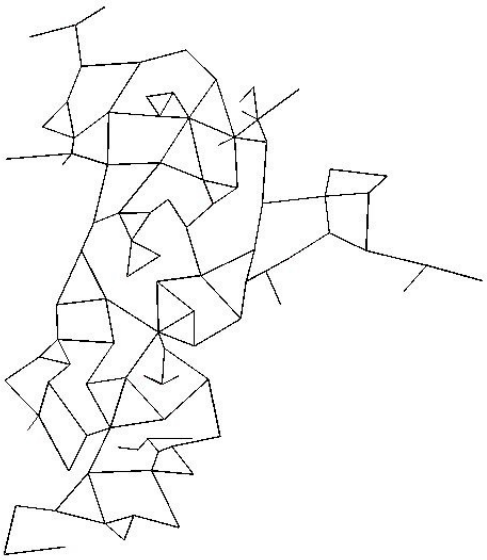
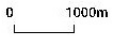
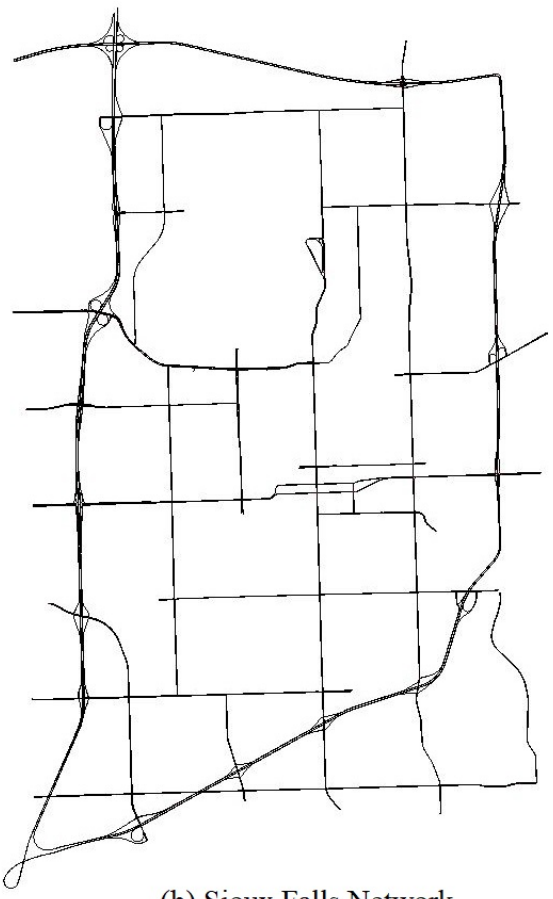

CAV fundamental diagram in micro and meso simulation
Micro
Meso
Flow (veh/hr)
Density (veh/km)
0
1000
2000
3000
4000
5000
6000
7000
0
50
100
150
200
250
300

Figure 2



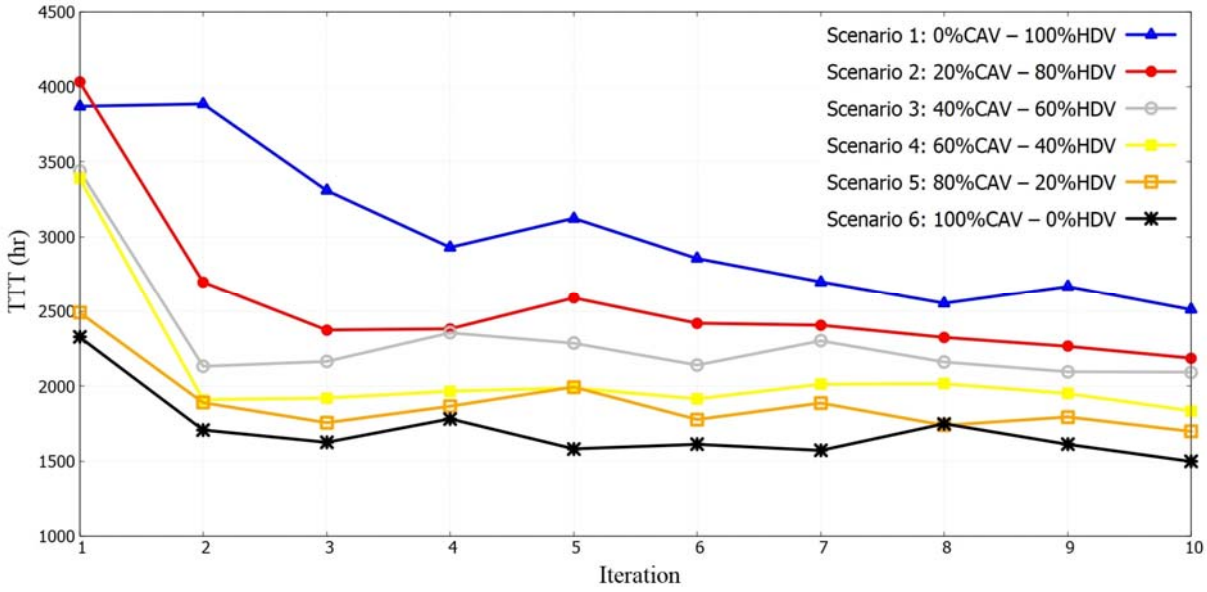
(a) Random Network





(b) Sioux Falls Network

Figure 3


Scenario 1: 0%CAV – 100%HDV
Scenario 2: 20%CAV – 80%HDV
Scenario 3: 40%CAV – 60%HDV
Scenario 4: 60%CAV – 40%HDV
Scenario 5: 80%CAV – 20%HDV
Scenario 6: 100%CAV – 0%HDV
TTT (hr)
Iteration
4500
4000
3500
3000
2500
2000
1500
1000
1
2
3
4
5
6
7
8
9
10
Figure 4

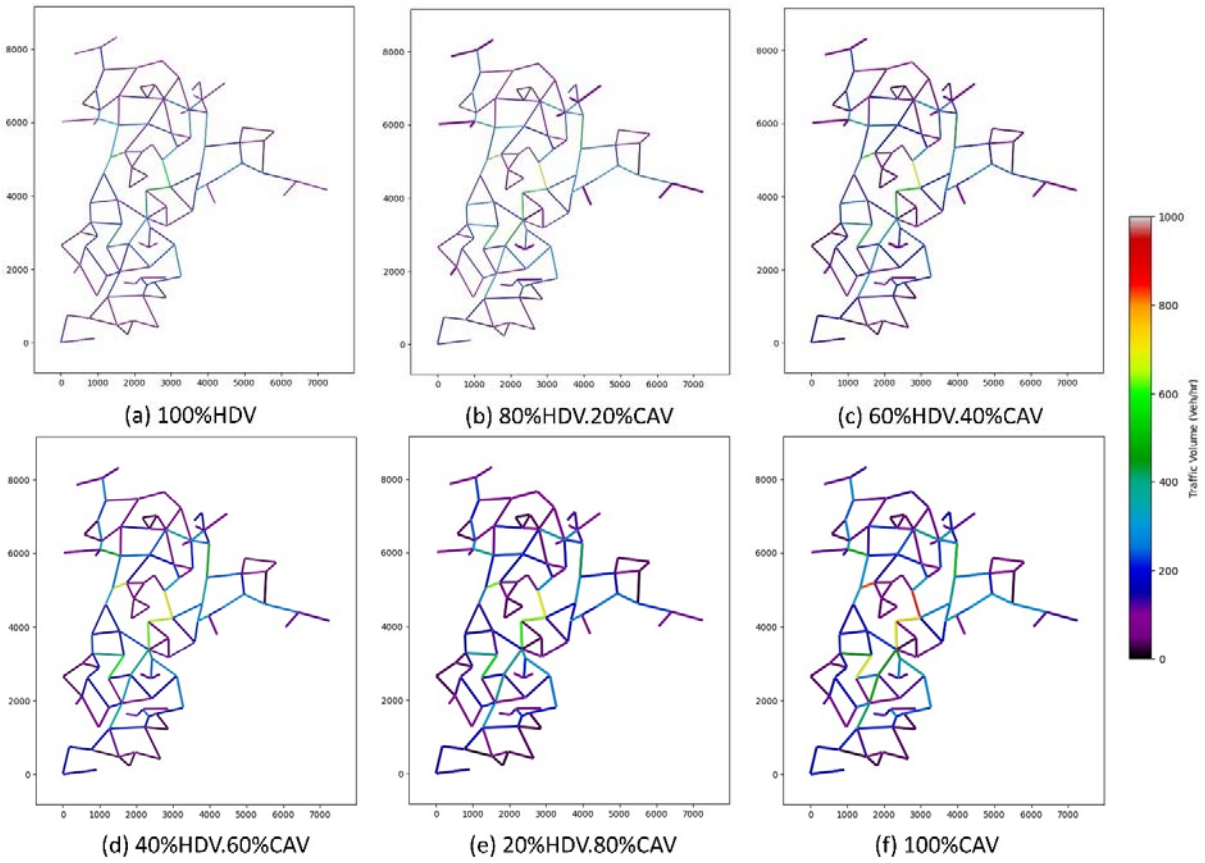

(a) 100%HDV
(b) 80%HDV.20%CAV
(c) 60%HDV.40%CAV
(d) 40%HDV.60%CAV
(e) 20%HDV.80%CAV
(f) 100%CAV
Traffic Volume (Veh/hr)
1000
800
600
400
200
0

Figure 5

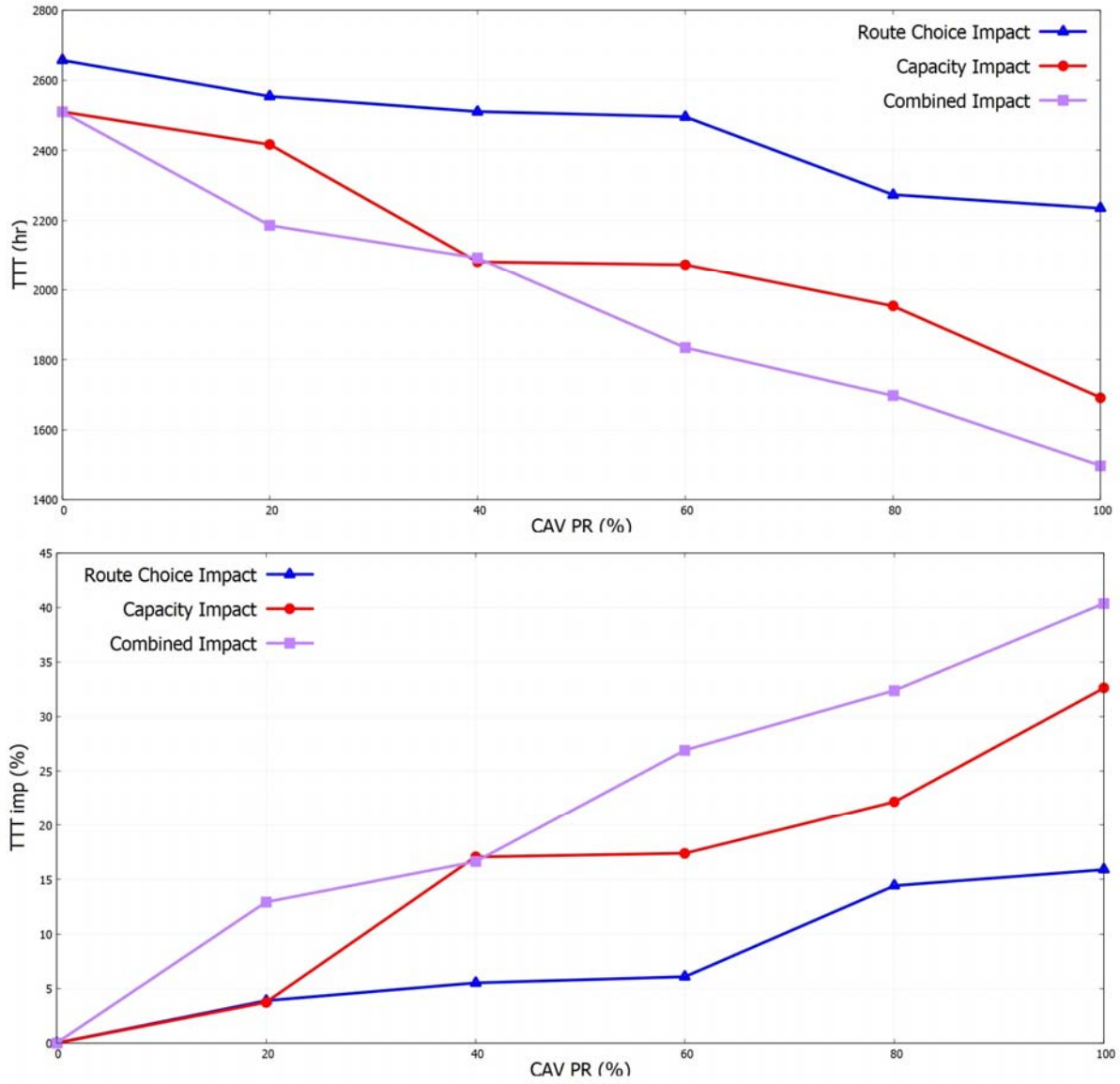

Route Choice Impact
Capacity Impact
Combined Impact
TTT (hr)
CAV PR (%)
Route Choice Impact
Capacity Impact
Combined Impact
TTT imp (%)
CAV PR (%)

Figure 6

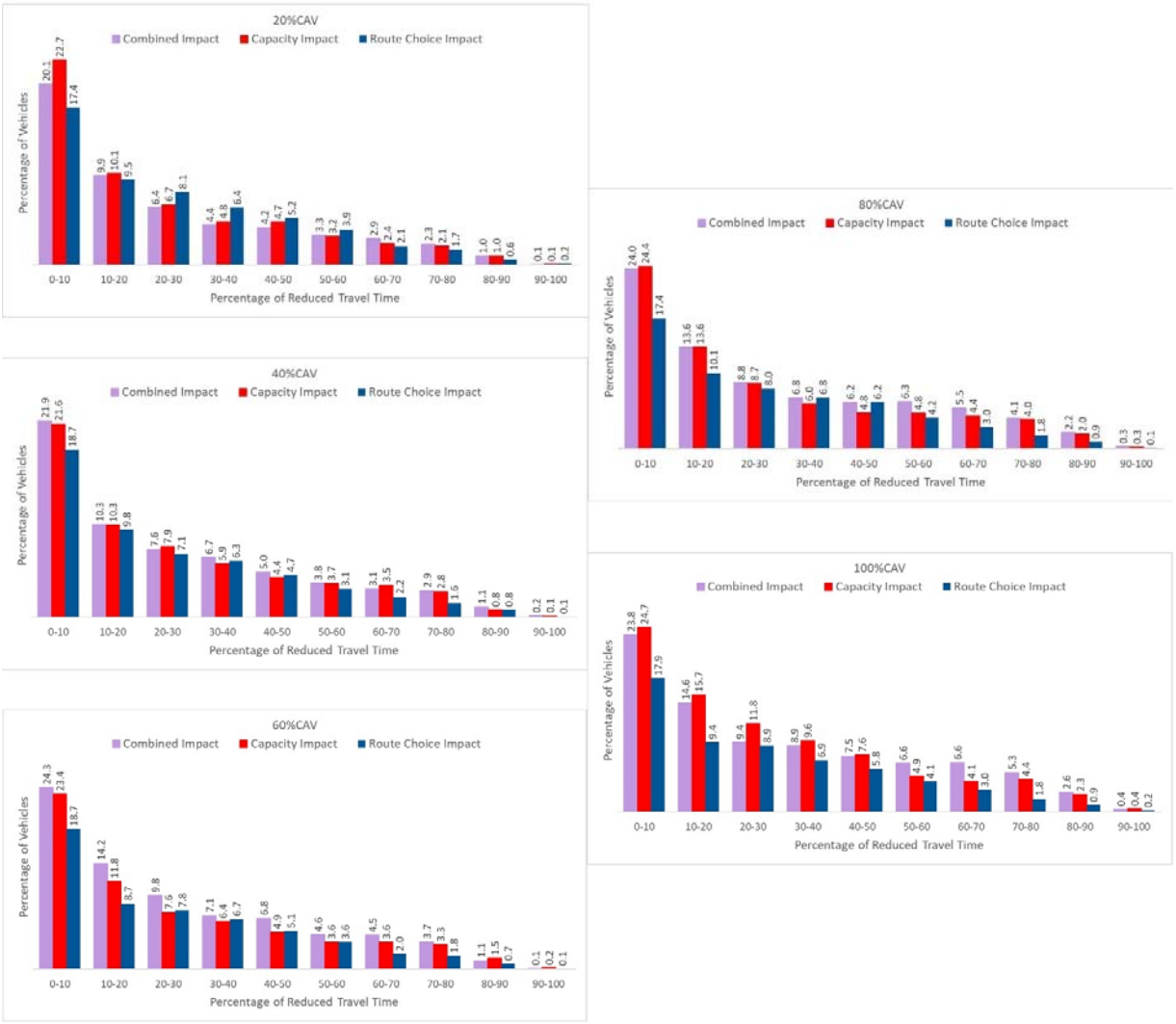

20%CAV
Combined Impact
Capacity Impact
Route Choice Impact
Percentage of Vehicles
20.1 23.7 17.4
9.9 10.1 9.5
6.4 6.7 8.1
4.4 4.8 6.4
4.2 4.7 5.2
3.3 3.2 3.9
2.9 2.4 2.1
2.3 2.1 1.7
1.0 1.0 0.6
0.1 0.1 0.2
0-10 10-20 20-30 30-40 40-50 50-60 60-70 70-80 80-90 90-100
Percentage of Reduced Travel Time
80%CAV
Combined Impact
Capacity Impact
Route Choice Impact
Percentage of Vehicles
24.0 24.4 17.4
13.6 13.6 10.1
8.8 8.7 8.0
6.8 6.0 6.8
6.2 4.8 6.2
6.3 4.8 4.2
5.5 4.4 3.0
4.1 4.0 1.8
2.2 2.0 0.9
0.3 0.3 0.1
0-10 10-20 20-30 30-40 40-50 50-60 60-70 70-80 80-90 90-100
Percentage of Reduced Travel Time
40%CAV
Combined Impact
Capacity Impact
Route Choice Impact
Percentage of Vehicles
21.9 21.6 18.7
10.3 10.3 9.8
7.6 7.9 7.1
6.7 5.9 6.3
5.0 4.4 4.7
3.8 3.7 3.1
3.1 3.5 2.2
2.9 2.8 1.9
1.1 0.8 0.8
0.2 0.1 0.1
0-10 10-20 20-30 30-40 40-50 50-60 60-70 70-80 80-90 90-100
Percentage of Reduced Travel Time
100%CAV
Combined Impact
Capacity Impact
Route Choice Impact
Percentage of Vehicles
23.8 24.7 17.9
14.6 15.7 9.4
9.4 11.8 8.9
8.9 9.6 6.9
7.5 7.6 5.8
6.6 4.9 4.1
6.6 4.1 3.0
5.3 4.4 1.8
2.6 2.3 0.9
0.4 0.4 0.2
0-10 10-20 20-30 30-40 40-50 50-60 60-70 70-80 80-90 90-100
Percentage of Reduced Travel Time
60%CAV
Combined Impact
Capacity Impact
Route Choice Impact
Percentage of Vehicles
24.3 23.4 18.7
14.2 11.8 8.7
9.8 7.6 7.8
7.1 6.4 6.7
6.8 4.9 5.1
4.6 3.6 3.6
4.5 3.6 2.9
3.7 3.3 1.8
1.1 1.5 0.7
0.1 0.2 0.1
0-10 10-20 20-30 30-40 40-50 50-60 60-70 70-80 80-90 90-100
Percentage of Reduced Travel Time

Figure 7

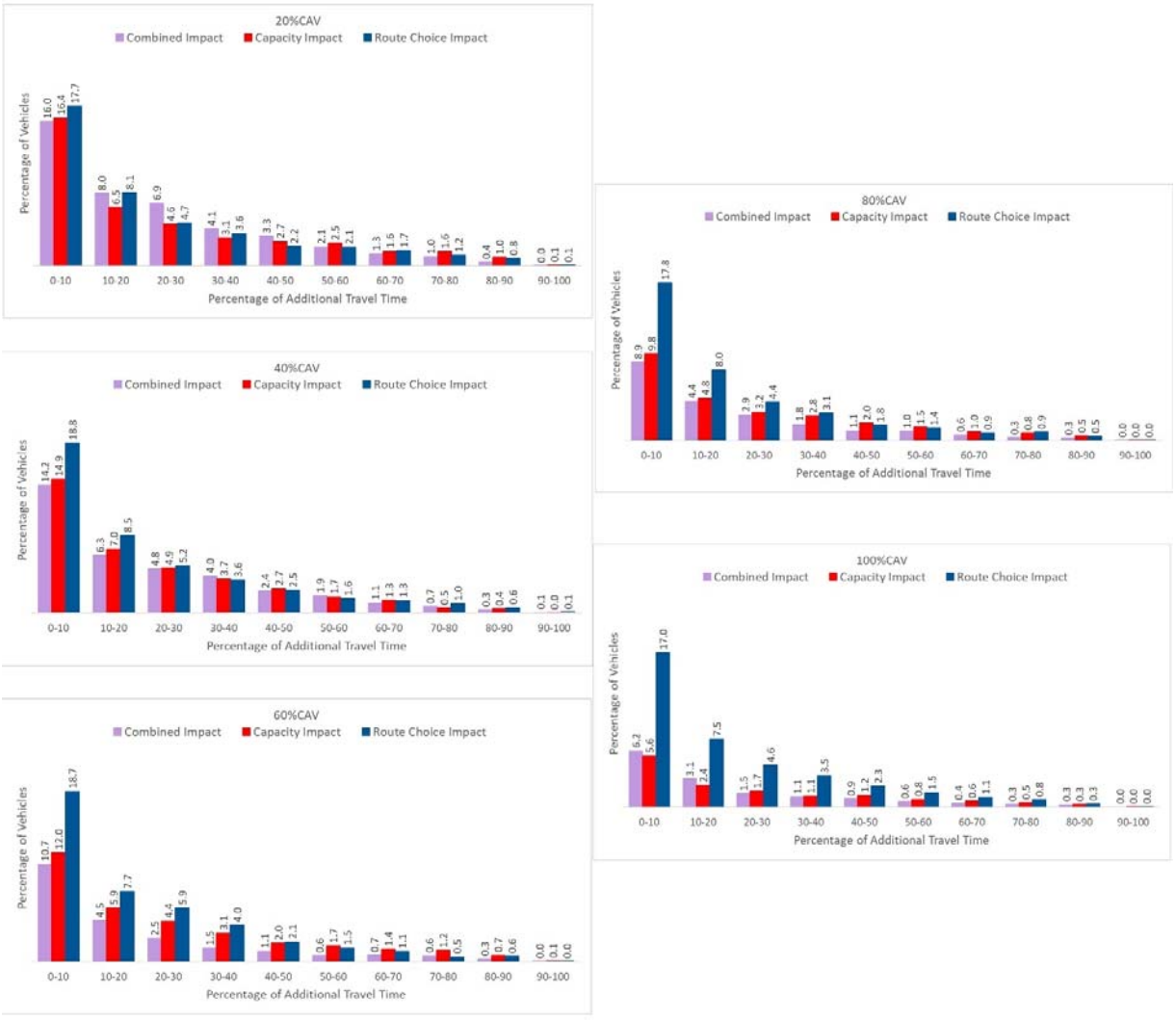

20%CAV
Combined Impact
Capacity Impact
Route Choice Impact
Percentage of Vehicles
16.0 16.4 17.7
8.0 6.5 8.1
6.9 4.6 4.7
4.1 3.1 3.6
3.3 2.7 2.2
2.1 2.5 2.1
1.3 1.6 1.7
1.0 1.6 1.2
0.4 1.0 0.8
0.0 0.1 0.1
0-10 10-20 20-30 30-40 40-50 50-60 60-70 70-80 80-90 90-100
Percentage of Additional Travel Time
40%CAV
Combined Impact
Capacity Impact
Route Choice Impact
Percentage of Vehicles
14.2 14.9 18.8
6.3 7.0 8.5
4.8 4.9 5.2
4.0 3.7 3.6
2.4 2.7 2.5
1.9 1.7 1.6
1.1 1.3 1.3
0.7 0.5 1.0
0.3 0.4 0.6
0.1 0.0 0.1
0-10 10-20 20-30 30-40 40-50 50-60 60-70 70-80 80-90 90-100
Percentage of Additional Travel Time
60%CAV
Combined Impact
Capacity Impact
Route Choice Impact
Percentage of Vehicles
10.7 12.0 18.7
4.5 5.9 7.7
2.5 4.4 5.9
1.5 3.1 4.0
1.1 2.0 2.1
0.6 1.7 1.5
0.7 1.4 1.1
0.6 1.2 0.5
0.3 0.7 0.6
0.0 0.1 0.0
0-10 10-20 20-30 30-40 40-50 50-60 60-70 70-80 80-90 90-100
Percentage of Additional Travel Time
80%CAV
Combined Impact
Capacity Impact
Route Choice Impact
Percentage of Vehicles
8.9 9.8 17.8
4.4 4.8 8.0
2.9 3.2 4.4
1.8 2.8 3.1
1.1 2.0 1.8
1.0 1.5 1.4
0.6 1.0 0.9
0.3 0.8 0.9
0.3 0.5 0.5
0.0 0.0 0.0
0-10 10-20 20-30 30-40 40-50 50-60 60-70 70-80 80-90 90-100
Percentage of Additional Travel Time
100%CAV
Combined Impact
Capacity Impact
Route Choice Impact
Percentage of Vehicles
6.2 5.6 17.0
3.1 2.4 7.5
1.5 1.7 4.6
1.1 1.1 3.5
0.9 1.2 2.3
0.6 0.8 1.5
0.4 0.6 1.1
0.3 0.5 0.8
0.3 0.3 0.3
0.0 0.0 0.0
0-10 10-20 20-30 30-40 40-50 50-60 60-70 70-80 80-90 90-100
Percentage of Additional Travel Time

Figure 8

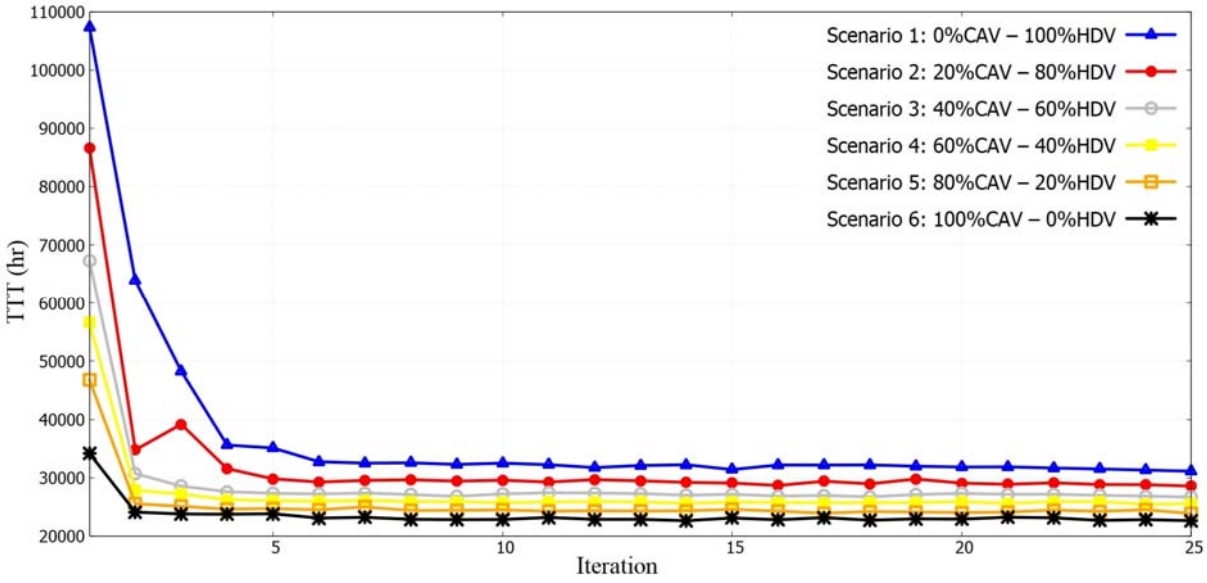

Scenario 1: 0%CAV – 100%HDV
Scenario 2: 20%CAV – 80%HDV
Scenario 3: 40%CAV – 60%HDV
Scenario 4: 60%CAV – 40%HDV
Scenario 5: 80%CAV – 20%HDV
Scenario 6: 100%CAV – 0%HDV
TTT (hr)
Iteration
110000
100000
90000
80000
70000
60000
50000
40000
30000
20000
5
10
15
20
25

Figure 9

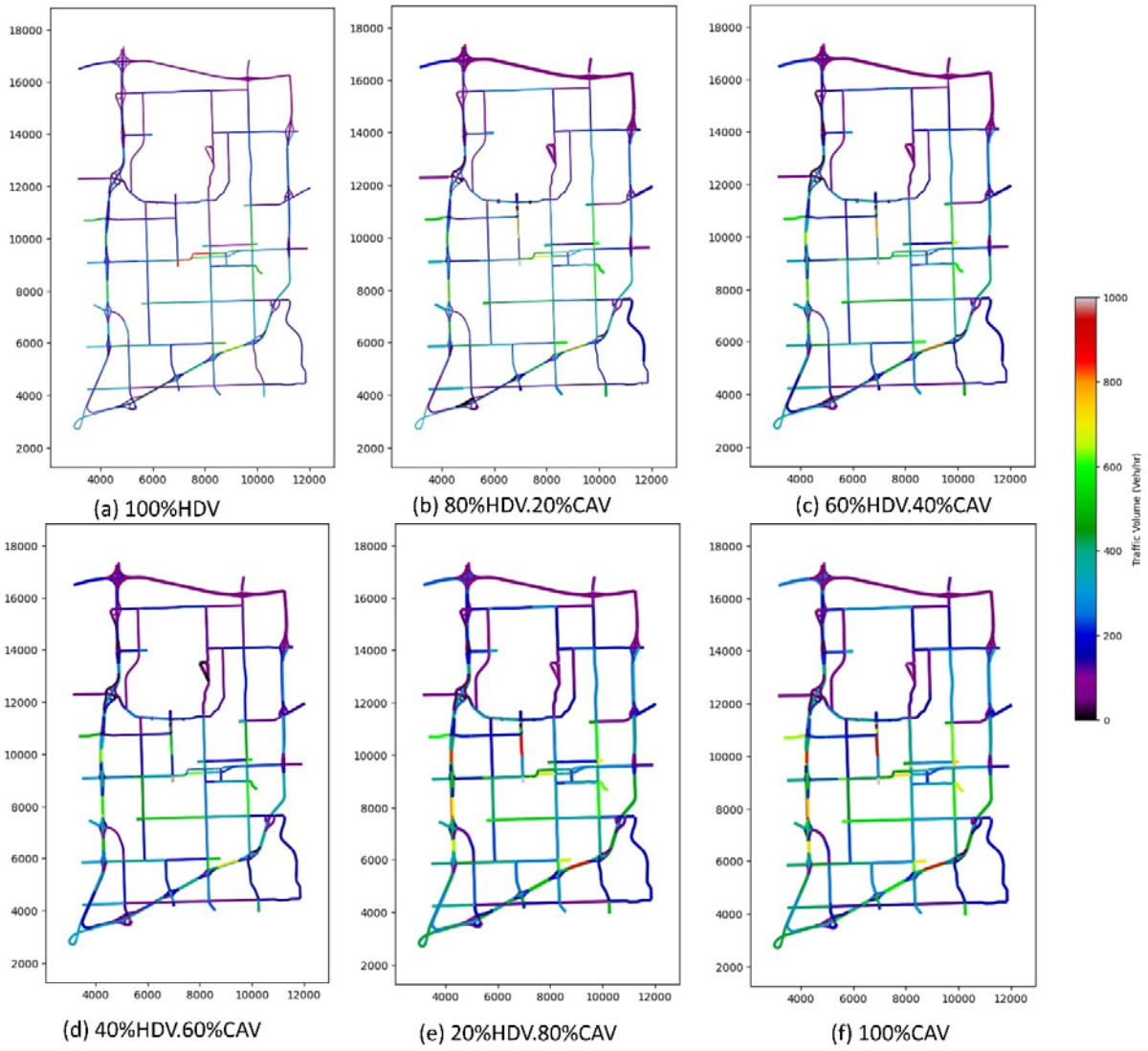

(a) 100%HDV
(b) 80%HDV.20%CAV
(c) 60%HDV.40%CAV
(d) 40%HDV.60%CAV
(e) 20%HDV.80%CAV
(f) 100%CAV
Traffic Volume (Veh/hr)
0
200
400
600
800
1000

Figure 10

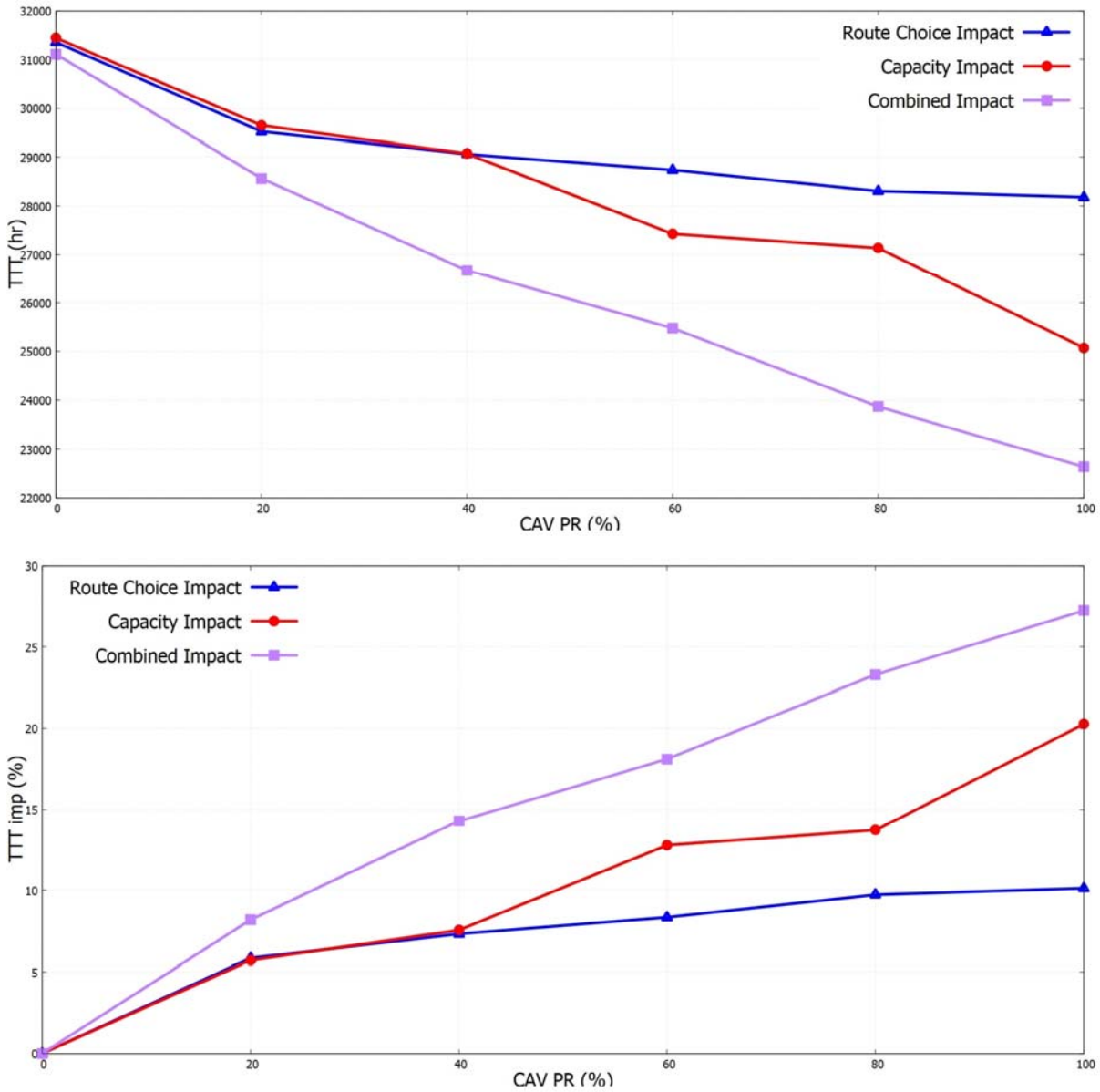

Route Choice Impact
Capacity Impact
Combined Impact
TTT (hr)
CAV PR (%)
TTT imp (%)

Figure 11

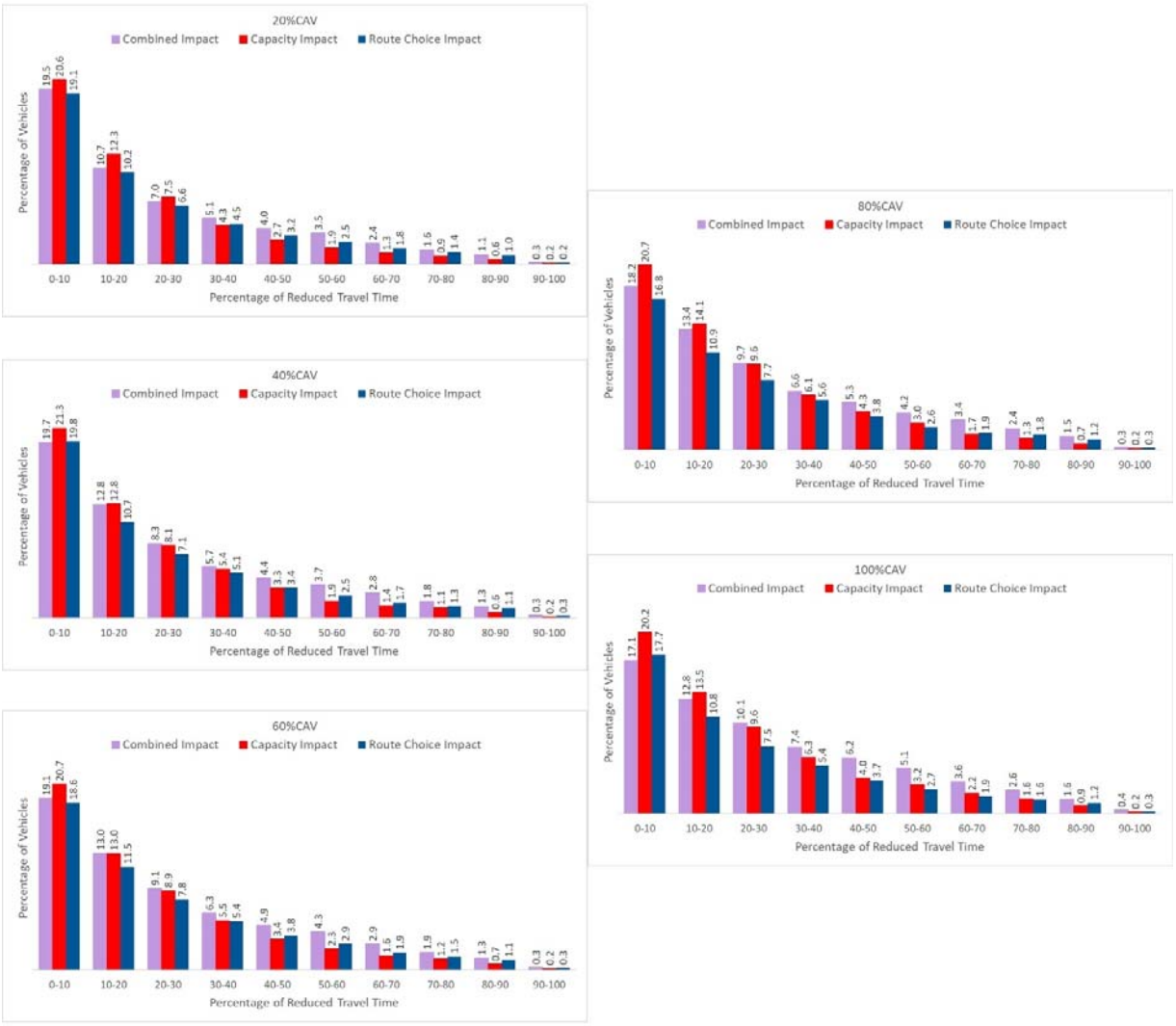

20%CAV
Combined Impact
Capacity Impact
Route Choice Impact
Percentage of Vehicles
19.5 20.6 19.1
10.7 12.3 10.2
7.0 7.5 6.6
5.1 4.3 4.5
4.0 2.7 3.2
3.5 1.9 2.5
2.4 1.3 1.8
1.6 0.9 1.4
1.1 0.6 1.0
0.3 0.2 0.2
0-10 10-20 20-30 30-40 40-50 50-60 60-70 70-80 80-90 90-100
Percentage of Reduced Travel Time
40%CAV
Combined Impact
Capacity Impact
Route Choice Impact
Percentage of Vehicles
19.7 21.3 19.8
12.8 12.8 10.7
8.3 8.1 7.1
5.7 5.4 5.1
4.4 3.3 3.4
3.7 1.9 2.5
2.8 1.4 1.7
1.8 1.1 1.3
1.3 0.6 1.1
0.3 0.2 0.3
0-10 10-20 20-30 30-40 40-50 50-60 60-70 70-80 80-90 90-100
Percentage of Reduced Travel Time
60%CAV
Combined Impact
Capacity Impact
Route Choice Impact
Percentage of Vehicles
19.1 20.7 18.6
13.0 13.0 11.5
9.1 8.9 7.8
6.3 5.5 5.4
4.9 3.4 3.8
4.3 2.3 2.9
2.9 1.6 1.9
1.9 1.2 1.5
1.3 0.7 1.1
0.3 0.2 0.3
0-10 10-20 20-30 30-40 40-50 50-60 60-70 70-80 80-90 90-100
Percentage of Reduced Travel Time
80%CAV
Combined Impact
Capacity Impact
Route Choice Impact
Percentage of Vehicles
16.3 20.7 16.8
13.4 14.1 10.9
9.7 9.6 7.7
6.6 6.1 5.6
5.3 4.3 3.8
4.2 3.0 2.6
3.4 1.7 1.9
2.4 1.3 1.8
1.5 0.7 1.2
0.3 0.2 0.3
0-10 10-20 20-30 30-40 40-50 50-60 60-70 70-80 80-90 90-100
Percentage of Reduced Travel Time
100%CAV
Combined Impact
Capacity Impact
Route Choice Impact
Percentage of Vehicles
17.1 20.2 17.7
12.8 15.5 10.8
10.1 9.6 7.5
7.4 6.3 5.4
6.2 4.0 3.7
5.1 3.2 2.7
3.6 2.2 1.9
2.6 1.6 1.6
1.6 0.9 1.2
0.4 0.2 0.3
0-10 10-20 20-30 30-40 40-50 50-60 60-70 70-80 80-90 90-100
Percentage of Reduced Travel Time

Figure 12

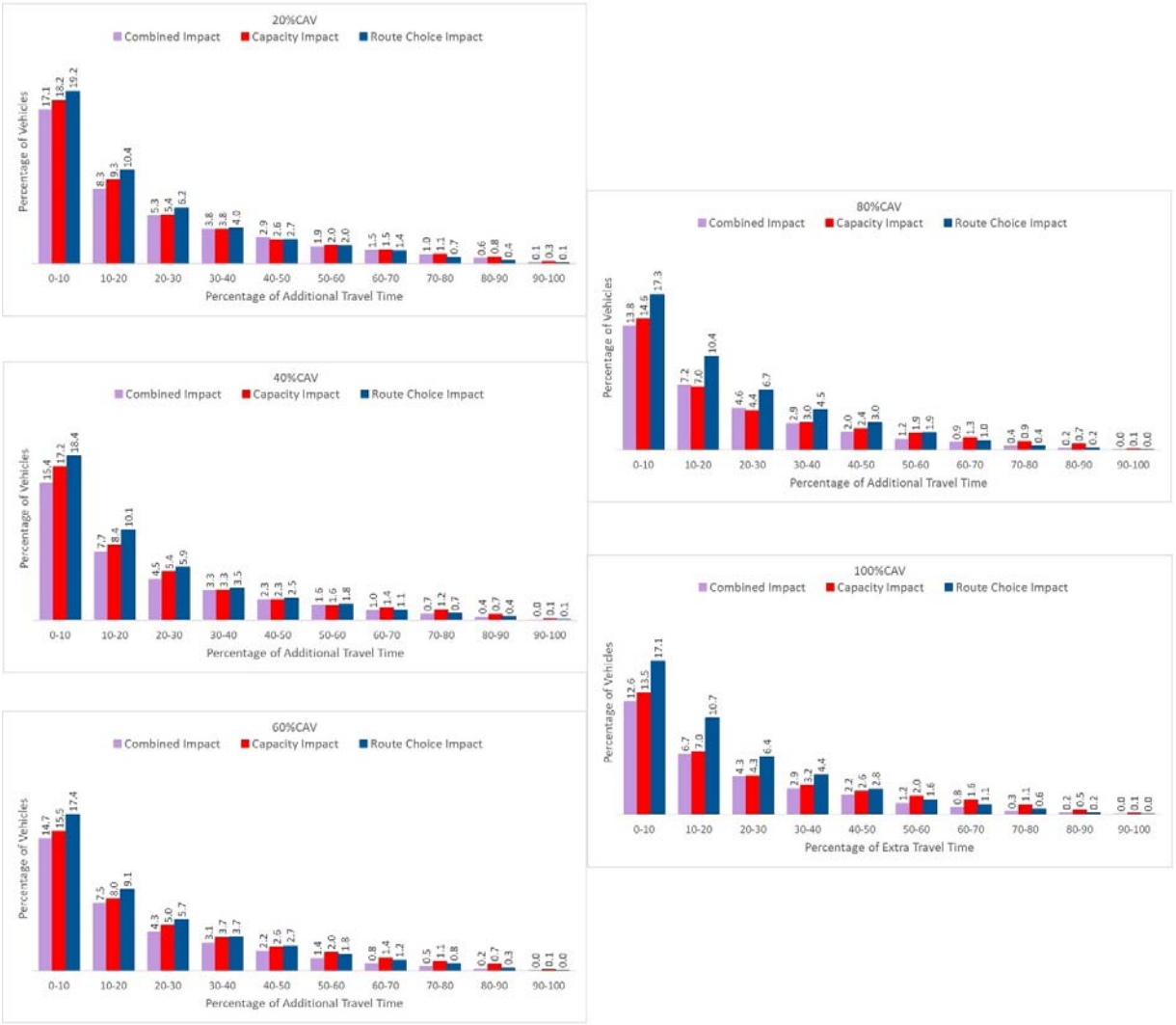

20%CAV
Combined Impact
Capacity Impact
Route Choice Impact
Percentage of Vehicles
17.1 18.2 19.2
8.3 9.3 10.4
5.3 5.4 6.2
3.8 3.8 4.0
2.9 2.6 2.7
1.9 2.0 2.0
1.5 1.5 1.4
1.0 1.1 0.7
0.6 0.8 0.4
0.1 0.3 0.1
0-10 10-20 20-30 30-40 40-50 50-60 60-70 70-80 80-90 90-100
Percentage of Additional Travel Time
40%CAV
Combined Impact
Capacity Impact
Route Choice Impact
Percentage of Vehicles
15.4 17.2 18.4
7.7 8.4 10.1
4.5 5.4 5.9
3.3 3.3 3.5
2.3 2.3 2.5
1.6 1.6 1.8
1.0 1.4 1.1
0.7 1.2 0.7
0.4 0.7 0.4
0.0 0.1 0.1
0-10 10-20 20-30 30-40 40-50 50-60 60-70 70-80 80-90 90-100
Percentage of Additional Travel Time
60%CAV
Combined Impact
Capacity Impact
Route Choice Impact
Percentage of Vehicles
14.7 15.5 17.4
7.5 8.0 9.1
4.3 5.0 5.7
3.1 3.7 3.7
2.2 2.6 2.7
1.4 2.0 1.8
0.8 1.4 1.2
0.5 1.1 0.8
0.2 0.7 0.3
0.0 0.1 0.0
0-10 10-20 20-30 30-40 40-50 50-60 60-70 70-80 80-90 90-100
Percentage of Additional Travel Time
80%CAV
Combined Impact
Capacity Impact
Route Choice Impact
Percentage of Vehicles
13.8 14.6 17.3
7.2 7.6 10.4
4.6 4.4 6.7
2.9 3.0 4.5
2.0 2.4 3.0
1.2 1.5 1.9
0.9 1.3 1.0
0.4 0.9 0.4
0.2 0.7 0.2
0.0 0.1 0.0
0-10 10-20 20-30 30-40 40-50 50-60 60-70 70-80 80-90 90-100
Percentage of Additional Travel Time
100%CAV
Combined Impact
Capacity Impact
Route Choice Impact
Percentage of Vehicles
12.6 13.5 17.1
6.7 7.0 10.7
4.3 4.3 6.4
2.9 3.2 4.4
2.2 2.6 2.8
1.2 2.0 1.6
0.8 1.6 1.1
0.3 1.1 0.6
0.2 0.5 0.2
0.0 0.1 0.0
0-10 10-20 20-30 30-40 40-50 50-60 60-70 70-80 80-90 90-100
Percentage of Extra Travel Time

Figure 13

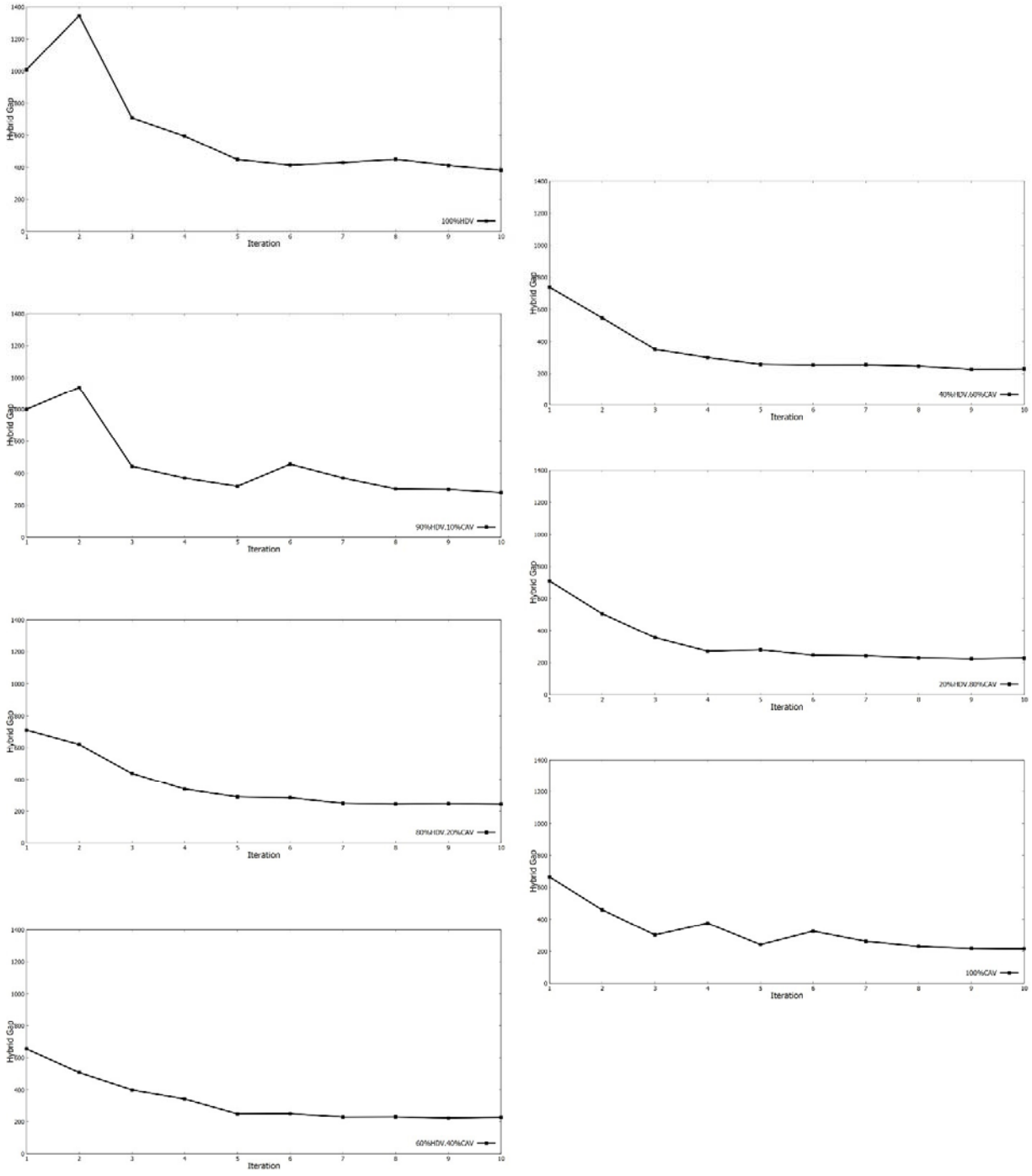

Hybrid Gap
Iteration
100%HDV
90%HDV,10%CAV
80%HDV,20%CAV
60%HDV,40%CAV
40%HDV,60%CAV
20%HDV,80%CAV
100%CAV

Figure 14

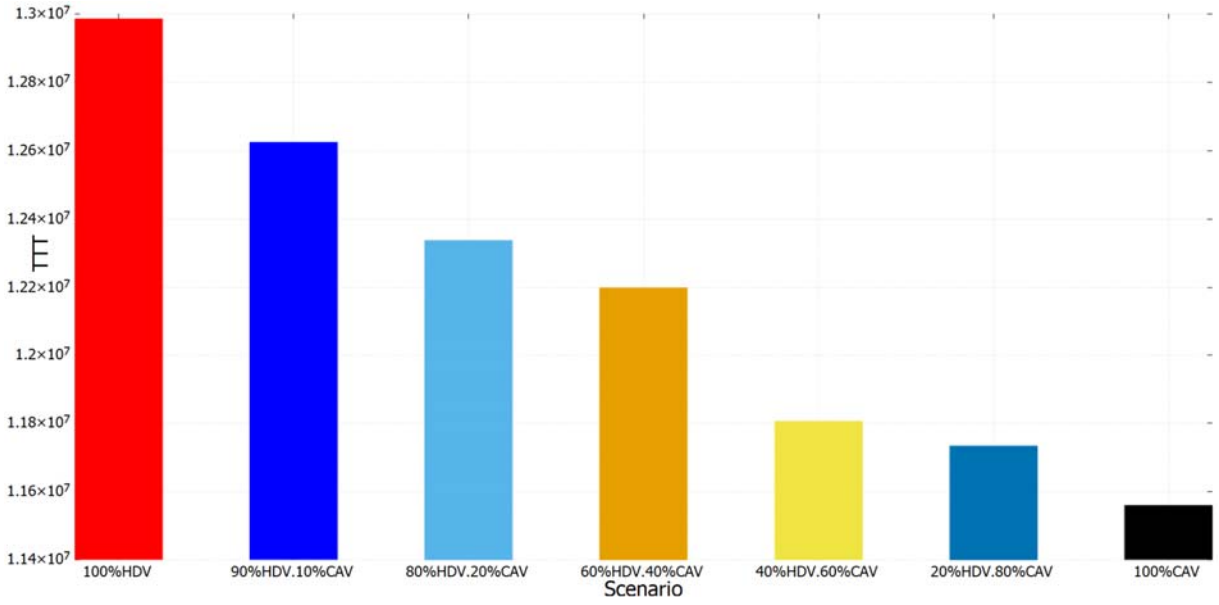

1.3×10^7
1.28×10^7
1.26×10^7
1.24×10^7
1.22×10^7
1.2×10^7
1.18×10^7
1.16×10^7
1.14×10^7
TT
100%HDV
90%HDV.10%CAV
80%HDV.20%CAV
60%HDV.40%CAV
40%HDV.60%CAV
20%HDV.80%CAV
100%CAV
Scenario

Figure 15

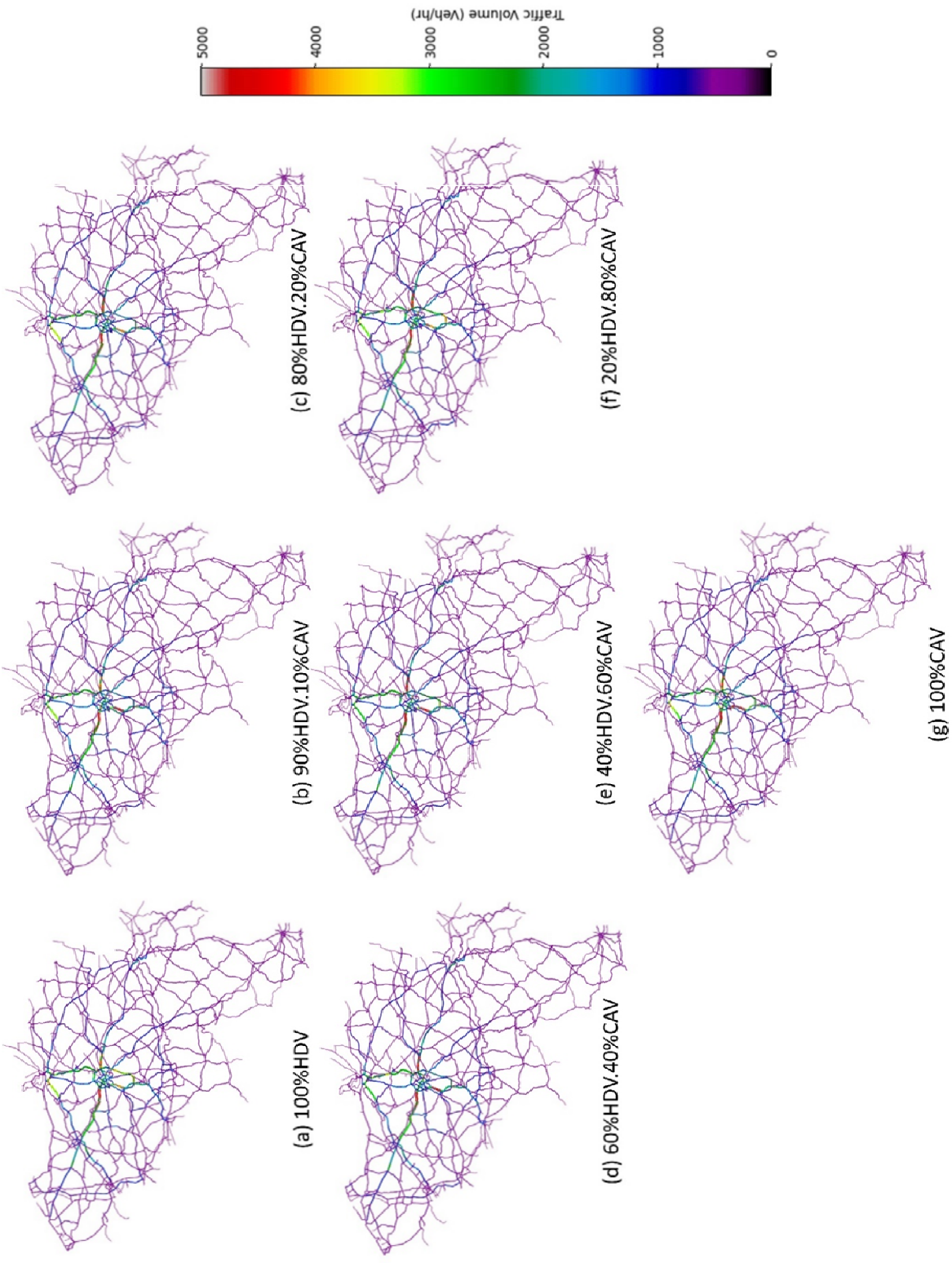

Traffic Volume (Veh/hr)
5000
4000
3000
2000
1000
0
(a) 100%HDV
(b) 90%HDV.10%CAV
(c) 80%HDV.20%CAV
(d) 60%HDV.40%CAV
(e) 40%HDV.60%CAV
(f) 20%HDV.80%CAV
(g) 100%CAV

Figure 16

Figure captions

Figure 1: Framework of the MS-TAP-M
Figure 2: HDVs and CAVs fundamental diagrams in micro and meso simulations
Figure 3: Test Networks
Figure 4: Convergence patterns for Random network
Figure 5: Traffic Volume of Random Network in different Penetration Rate of CAVs
Figure 6: Impact of CAVs on TTT for Different Setting of Route Choice and Driving Behavior (Random Network)
Figure 7: Travel Time Heterogeneity (Reduced Travel Time) (Random Network)
Figure 8: Travel Time Heterogeneity (Additional Travel Time) (Random Network)
Figure 9: Convergence patterns for Sioux Falls network
Figure 10: Traffic Volume of Sioux Falls Network in different Penetration Rate of CAVs
Figure 11: Impact of CAVs on TTT for Different Setting of Route Choice and Driving Behavior (Sioux Falls Network)
Figure 12: Travel Time Heterogeneity (Reduced Travel Time) (Sioux Falls Network)
Figure 13: Travel Time Heterogeneity (Additional Travel Time) (Sioux Falls Network)
Figure 14: Convergence patterns for Belgium network
Figure 15: Total travel time in different penetration rate of CAVs (Belgium Network) (min)
Figure 16: Traffic Volume of Belgium Network in different Penetration Rate of CAVs